UserCom
2/2000

Information for users of
METTLER TOLEDO thermal analysis systems

Dear Customer
UserCom is becoming more and more popular. In the last edition, we made a number of improvements to the layout and have now decided to print a Spanish version in addition to the English, German and French editions.
On the last page, we would like to introduce the METTLER TOLEDO editorial team. The name of the author is now noted along with the title of each article.

12

Interpreting DSC curves; Part 2: Isothermal measurements

J. Widmann

Isothermal DSC measurements are used for the following applications:
- crystallization processes including polymorphism,
- desorption, vaporization and drying,
- chemical reactions such as autoxidation, polymerization or thermal decomposition.

Isothermal DSC measurement curves are usually easier to interpret than dynamic measurements curves (UserCom11):
- an important advantage of isothermal measurements is that an effect can be observed almost in isolation (other effects occur at other temperatures).
- changes in the heat capacity of the sample of course remain undetected, and the baselines are exactly horizontal (except in the transition range). The heat capacity can however be measured with quasi-isothermal methods such as the isothermal step method [1], or temperature modulated DSC (ADSC), in which the temperature is varied slightly around the mean value [2].
- All isothermal DSC curves flatten off asymptotically to 0 mW at the end of the reaction.

Contents

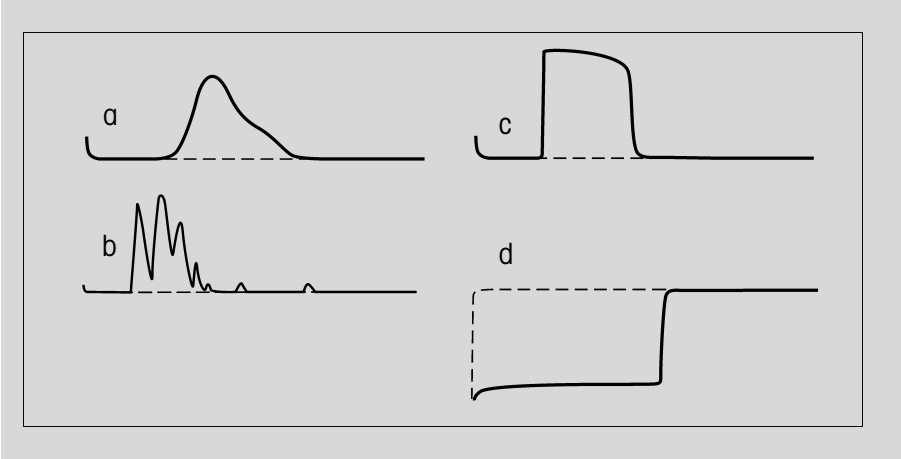

Fig. 1. Isothermal physical transitions; a: crystallization of a polymer, e.g. polypropylene cooled from the melt, T_{iso} = 130 °C (often with a shoulder, as shown); b: crystallization of a pure metal; c: enantiotropic reverse transition of the high temperature form to the low temperature modification (the crystallization of the melt of a pure substance consisting of individual droplets would look similar); d: evaporation of a solvent ca. 10 °C below the boiling point in a sample pan with a 1 mm hole in the lid. At constant temperature, the rate of crystallization of a substance that crystallizes well (b), and the evaporation rate of the solvent (d) remain practically constant until the end of the transition.

Strictly speaking, only the DSC furnace is isothermal. The sample itself is however isoperibolic, i.e. measured at constant furnace temperature, because it is not coupled directly to the isothermal furnace, but indirectly via the thermal resistance of the DSC sensor. For instance, with a heat flow of 10 mW and a thermal resistance of ca. 0.04 $K \cdot mW^{-1}$, the temperature of the sample differs by about 0.4 K from the temperature of the furnace. If the DSC signal decreases to zero during the course of the effect, then the sample temperature is exactly the same as the furnace temperature.

There are two ways to raise the sample as rapidly as possible to the temperature required for the isothermal measurement:

1. Preheat the measuring cell for several minutes at the desired temperature and then introduce the sample pan with the automatic sample robot. With this technique, the sample reproducibly reaches the programmed temperature within half a minute to an accuracy of 0.1 K. This applies to the low mass Al pans and to the standard Al pans; with heavier pans, e.g. high pressure crucibles, temperature equilibration naturally takes longer.
   If a sample robot is not available, you can, with a bit of practice, introduce the pan manually even more rapidly. If the automatic furnace lid is not installed, hold the manual furnace lid with a second pair of tweezers in one hand while you introduce the sample with the other hand. Make sure that the lid cools down as little as possible. The manual method allows a defined thermal pretreatment of the sample.
   Examples are:
   - A sample is shock-cooled in liquid nitrogen and then allowed to crystallize in the DSC at 0 °C.
   - A sample is melted at 200 °C and then allowed to crystallize in the DSC at 130 °C.

   In our laboratory we use an old DSC20 measuring cell as an accurate furnace for thermal pretreatment.
2. Insert the sample and heat the measuring cell to the desired temperature at a linear rate. The advantage of this method is that the sample can be reproducibly subjected to (almost) any preprogrammed thermal history (an advantage for routine measurements). The disadvantage is that it can take minutes until the desired temperature is reached and has stabilized (longer transition period). In addition, you are limited to the maximum heating and cooling rates of the measuring cell.

You may want to evaluate the measured reaction free of any disturbances caused by the transition from the dynamic to isothermal state. You can do this by correcting the measurement curve, either by deconvolution, or better still, by subtracting the measurement curve of an inert sample with the same heat capacity measured with the same method (possibly a second measurement of the reacted sample, see Fig. 5).

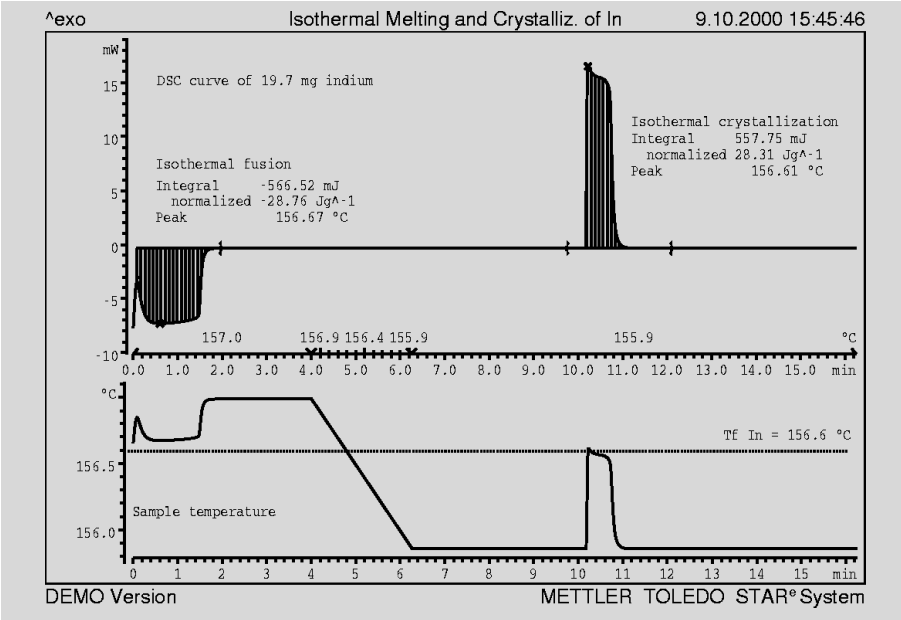

Fig. 2. The indium sample was put in the measuring cell that had been preheated to 157.0 °C. The sample immediately began to melt. Afterward it was cooled to 155.9 °C at 0.5 K/min. Isothermal crystallization begins after about 4 minutes. The sample temperature is displayed below. Because of the slight thermal resistance between the DSC sensor and the indium sample, the measured melting temperature is 0.06 K higher than the crystallization temperature.

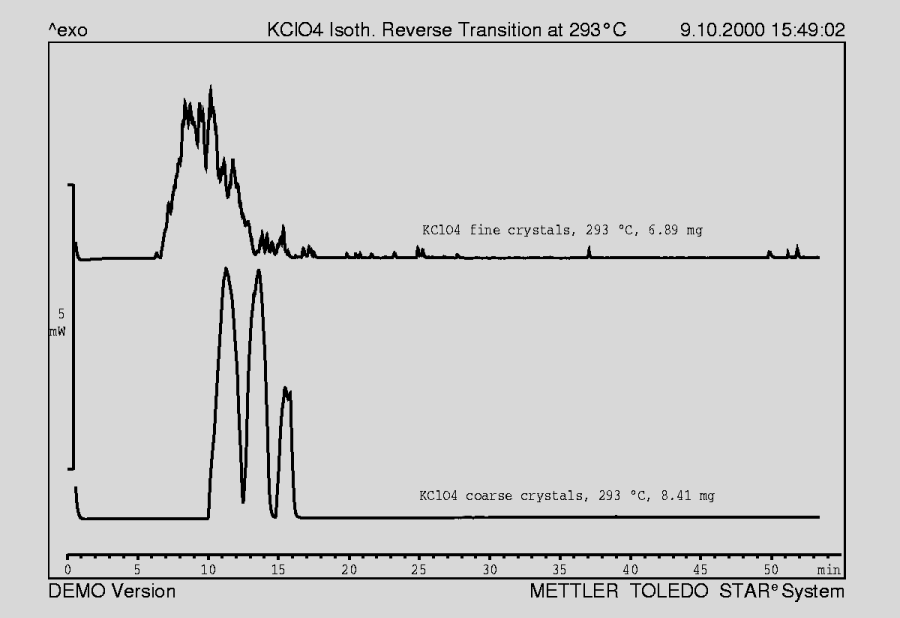

Fig. 3. The enantiotropic reverse transition of the high temperature form of potassium perchlorate at 7 K below the equilibrium temperature. The kinetics shown by the large number of fine crystals (above) is completely different to that of the small number of coarse crystals (below). Particularly fine crystals have an induction period of almost an hour. Samples of extremely fine crystals exhibit an almost smooth bell-shaped curve because of the very large number of individual particles (statistics).

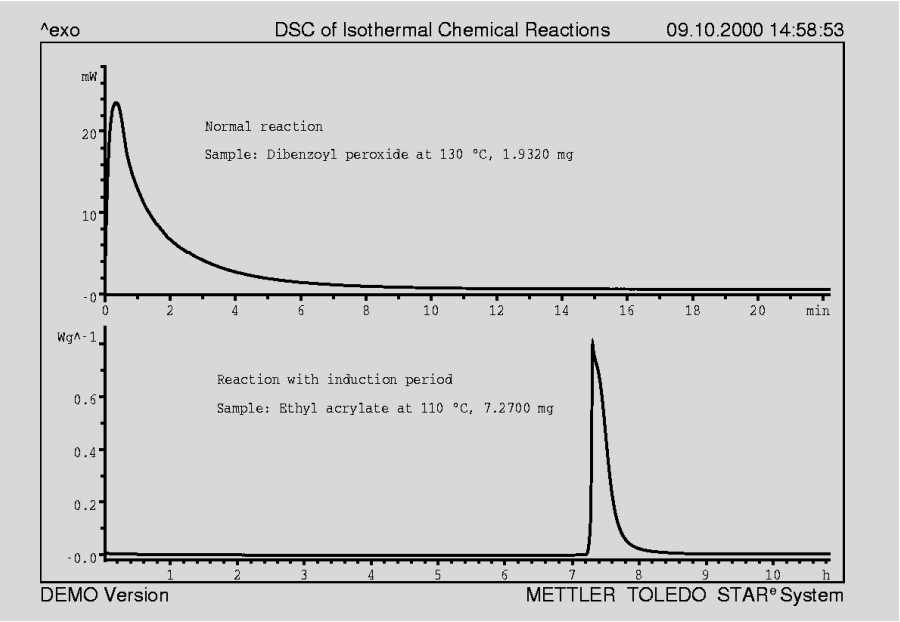

Fig. 4. Above: the "normal" course of the decomposition reaction of dibenzoyl peroxide dissolved in dibutyl phthalate measured in an Al pan with a 50 µm hole in the lid. The reaction rate is greatest at the beginning of the reaction when the concentration of unreacted material is highest. Afterward, the reaction falls off asymptotically to zero.
Below: an example of a reaction at 110 °C with an induction period of more than 7 hours. During the induction period, nothing appears to happen to the ethyl acrylate (in fact a stabilizer is used up). After this, the polymerization reaction then rapidly reaches the maximum rate.

Physical transitions

- Isothermal crystallization below the melting point (Fig. 1a: polypropylene at 130 °C, Fig. 2 above: indium at 155.9 °C). In comparison to dynamic cooling with relatively rapid cooling rates, larger crystals with fewer flaws are formed.
- Isothermal melting (Fig. 2, above left). With several isothermal steps, you can carefully approach the temperature of the thermodynamic equilibrium of the liquid and solid phases (melting and crystallization rate = 0, i.e. heat flow =0).
- Isothermal monotropic transition below the melting point of the metastable modification. In this way, you can transform the sample completely to the stable form, for example in order to determine its heat of fusion.
- Isothermal enantiotropic reverse transition below the equilibrium temperature, thereby gaining an insight into the bizarre kinetic behavior of the sample (Fig. 3).
- Isothermal evaporation (Fig. 1d) below the boiling point or sublimation below the melting temperature. This allows you to completely remove a volatile component and afterward measure the residue dynamically.

Chemical reactions

A so-called "normal" chemical reaction begins as soon as the reaction temperature is reached. It becomes slower and slower as the concentration of the starting materials decreases (Fig. 4, above). Autoaccelerating reactions, i.e. autocatalytic reactions, or reactions inhibited by the addition of stabilizers, have a significant induction period (Fig. 4, below) in which nothing appears to happen (the DSC signal is certainly less than about 0.1 mW). Afterward, the reaction rate increases rapidly to its maximum value, after which it decreases just like in a "normal" reaction.

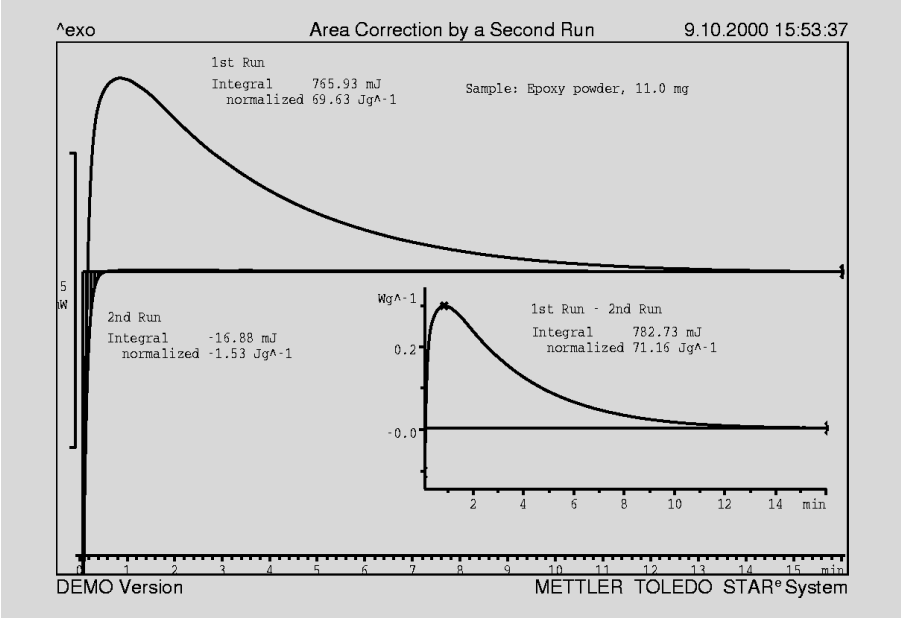

Fig. 5. Above left: the curing reaction of an epoxy resin at 190 °C is shown. The heat of reaction is 69.6 J/g using a horizontal baseline. The second measurement run afterward has an area of –1.5 J/g. The total area (i.e. the difference) is therefore 71.1 J/g. Below right: the difference curve (1st run – 2nd run) is displayed. The curve corrected in this way has an area of 71.2 J/g.

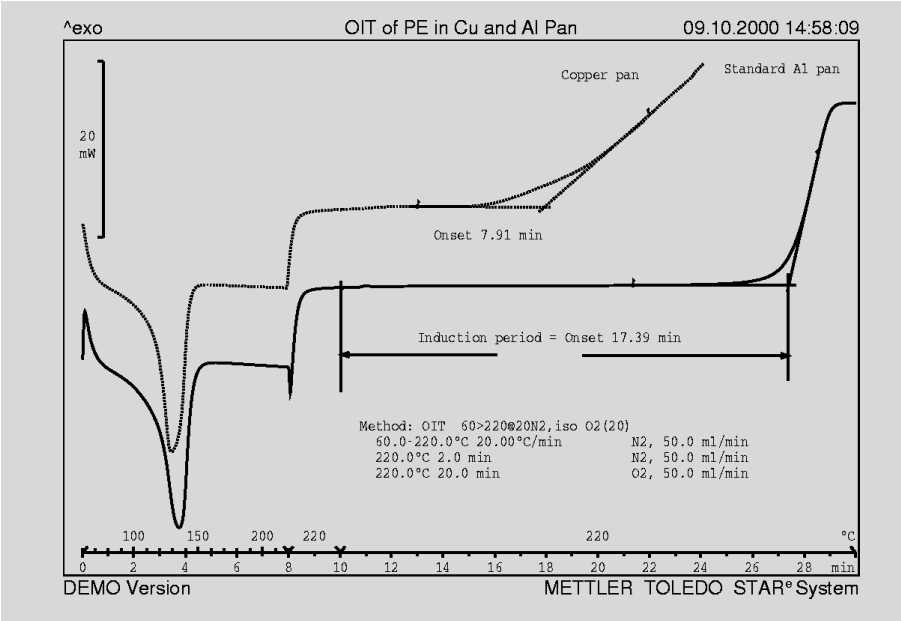

Fig. 6. Determination of the oxidative stability according to standards such as ASTM D3895-80, EN 728-97, ISO 11357-6. The sample is heated dynamically to the desired temperature in an inert atmosphere (N_2). There then follows a stabilization period of 2 minutes after which the measuring cell is purged with oxygen and measurement of the induction period begins.
Sample: polyethylene, Hostalen GM 5040 T12, ca. 12 mg. Measurement temperature: 220 °C
In the case of electrical insulation material, which is of course in contact with copper, the induction time of 17.4 minutes obtained with an aluminum pan is compared with the result using a copper pan. The value of 7.91 minutes demonstrates the unfavorable influence of the redox catalyst copper on the oxidative degradation of polyethylene.

Isothermal measurements are excellent for the detection of autoaccelerating processes. From the safety point of view, these are important to investigate but are otherwise difficult to measure. They can hardly be detected with a dynamic temperature program. For the initial isothermal measurements, we recommend a temperature that is about 40 K below the onset of the dynamic measurement.
The OIT (Oxidation Induction Time) is one of the most frequently performed isothermal measurements. It is used to compare the oxidative stability of polyolefines (Fig. 6) or petroleum in the presence of oxygen. The measurement is very often terminated on reaching a threshold value of 5 mW since usually only the induction time, i.e. the onset, is of interest. Vaporization of part of the sample at the measurement temperature of around 200 °C can be prevented by performing the measurement under increased pressure, e.g. at 3 MPa in a pressure DSC.
Thermosetting resins are often cured isothermally and the resulting glass transition temperature determined afterward.
Compared with dynamic measurements, isothermally measured reaction peaks provide a direct and clear insight into the kinetics of processes.

Literature

[1] *H. Staub und W. Perron, Analytical Chemistry 46 (1974) p 128*

[2] *METTLER TOLEDO ADSC software datasheet*

New in our sales program

Crucible brochure

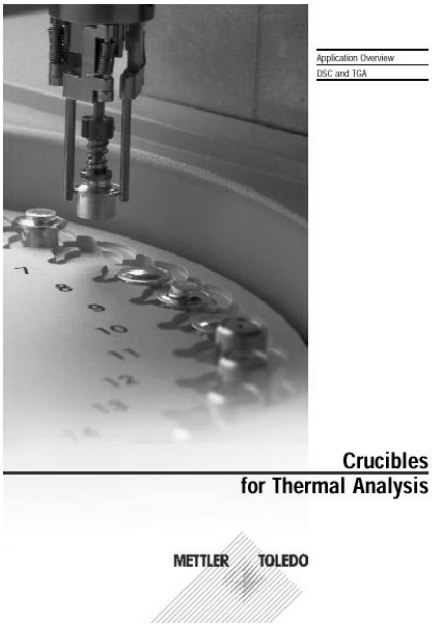

The new "Crucibles for Thermal Analysis" brochure describes the entire range of METTLER TOLEDO crucibles. The aim is to help you find the best crucible for your application as quickly and easily as possible.

There is a detailed description of each crucible together with information about its specific use and application. A comprehensive table helps you choose the right crucible.

Example: The light aluminum crucible, 20 µl
The light aluminum crucible has the shortest signal time constant, especially when using helium as a purge gas. It is particularly suitable for measuring polymer films, disks and powders - the samples are pressed down tightly against the base of the crucible.
It is less suitable for liquid samples because the liquids might be squeezed out of the crucible on sealing.
The narrow space between the crucible and the lid leads to the formation of a self-generated atmosphere. Piercing the lid beforehand allows contact with the atmosphere.
A special die set is required for the sealing press.

(English: 51 724 175, German: 51 724 174, , French: 51 724 176,
Spanish: 51 724 177, Italian: 51 724 178)

Automatic liquid nitrogen refilling system

You can work around the clock with the new automatic liquid nitrogen refilling system. This has advantages when used with the automatic sample robot, and is also useful for measurements performed over an extended period of time, e.g. with temperature modulated DSC (ADSC).
The automatic refilling system consists of a modified standard liquid nitrogen Dewar with an integrated filling level sensor, several magnetic valves and a new electronics control system. The automatic refilling system is connected directly to the liquid nitrogen valve (3) of the DSC module. The standard liquid nitrogen Dewar is installed on the inlet side of the refilling system.
As soon as the filling level sensor (1) of the automatic refilling system senses that the liquid nitrogen level is too low, it opens the valve on the inlet side (2) and pumps in liquid nitrogen until a predefined level is again reached.
Because this filling operation is also performed under pressure, the DSC module continues to work without interruption, and no measurement data is ever lost.

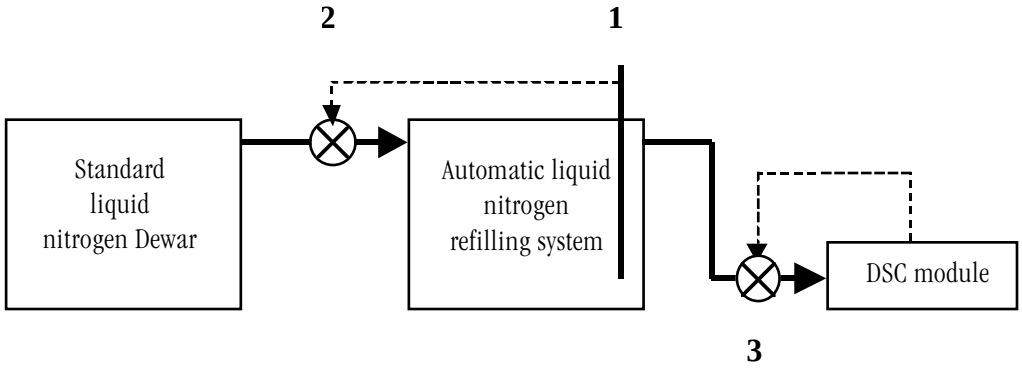

Characterization of petroleum products with DSC

J.M. Létoffé. Laboratoire de Thermodynamique Appliquée. INSA 69621. Villeurbanne Cedex. France

Introduction

Conventional fuel is obtained exclusively from petroleum or crude oil. Petroleum is primarily a mixture of 6 different classes of substances. The composition of the mixture is specific to the region where the oil occurs and consists of

- straight-chain n-alkanes (C_nH_{2n+2}) with molar masses between 16 and 300 g/mol
- branched-chain alkanes (iso-alkanes)
- cycloalkanes
- aromatics
- sulfur-containing compounds
- polycyclic and heterocyclic resins as well as bitumens with molar masses of about 1000 g/mol.

Distillation of the crude oil yields various fractions, which are classified as follows: low boiling fractions, e.g. gasoline (petrol), aviation gasoline, naphtha; higher boiling fractions, e.g. fuel or heating oil and diesel; and high boiling fractions (heavy oil and lubricating oils). The residue after distillation is known as bitumen (or asphalt).

In the liquid state, the distillate appears macroscopically as a single-phase mixture. On cooling, crystals are formed, i.e. a multiphase mixture is obtained. The separation of crystalline material is undesirable and leads to a number of problems:

1. Crystallized material separates out forming a sediment. This is often a problem, especially for the storage of diesel and heating oils.
2. Crystallized material is retained in filters, which can lead to blockages.
3. Bitumen (asphalt) products are mainly used for surfacing roads. Crystallization causes the surface to become brittle and results in the formation of cracks.

Hydrocarbon distillates consist primarily of complex hydrocarbon compounds and crystallizable fractions. The former are partially liquid at room temperature and exhibit a glass transition at low temperatures. The glass transition temperatures of the liquid constituents depend on the petroleum distillate. Typical values are -30 °C for bitumen, -130 °C for diesel and -150 °C for gasoline. The proportion of the crystallizable fractions is between 0% and 10% for bitumen, between 5% and 25% for fuel oil and up to 40% for crude oil. The chemical structure of the crystals depends on the distillate. With fuel oils, n-alkanes with 10 to 28 carbon atoms crystallize out, with bitumen n-alkanes with 20 to 60 carbon atoms; and with crude oil n-alkanes with 5 to 60 carbon atoms. Lightly branched iso-alkanes and cycloalkanes are also present.

Characterization of petroleum products with DSC

Petroleum products are usually characterized by their glass transition temperature and their melting behavior. The measurement of these parameters is easily performed by DSC. A typical temperature program for the analysis of petroleum derivatives begins by cooling the sample at 10 K/min from room temperature to -100 °C (for heavy hydrocarbon compounds) or to -150 °C (for light hydrocarbon compounds, e.g. kerosene, gasoline). Afterward the sample is heated linearly at 5 K/min up to final temperatures of typically 50 °C (for fuel oils such as light heating oil or diesel), 80 °C (crude oil), 100 °C (heavy oil) and 120 °C (bitumen). Figure 1 shows the corresponding heating curves for different samples. Various effects can be ob-

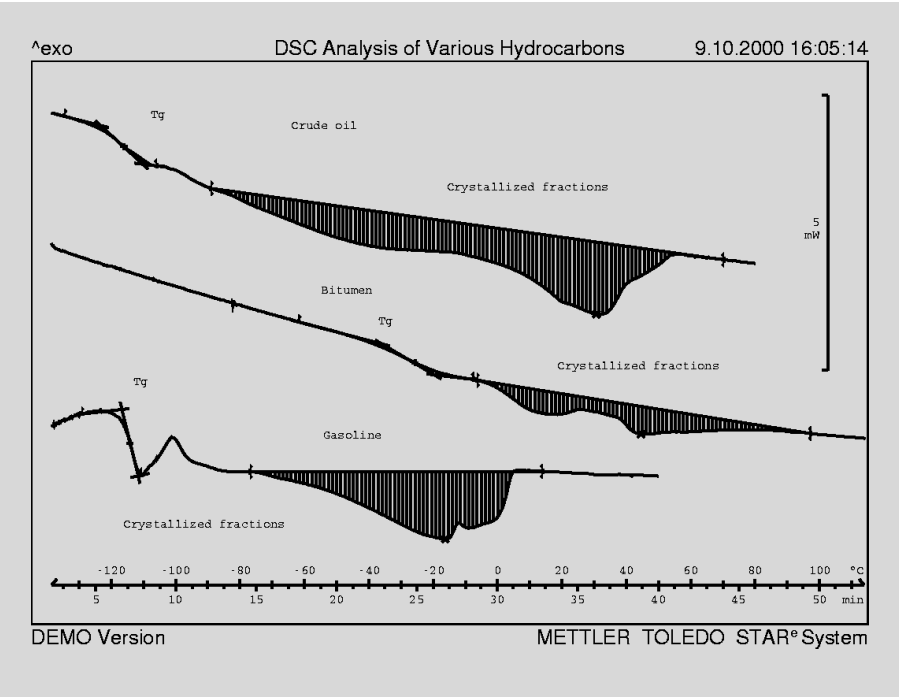

Fig. 1. DSC curves of different petroleum distillates

served. The marked increase of the heat capacity at low temperatures (step in the heat flow curve) is caused by the glass transition. Very often, part of the sample then crystallizes out (usually iso-alkanes), causing an exothermic peak. The melting of the various crystals can lead to several relatively broad, endothermic peaks. The shape of the peak mirrors the size and weight distribution of the crystals and is characteristic of a particular distillate or particular crude oil.

For medium distillates (gasoline, heating oil), $\Delta H(T)$ can be described by a third order polynomial [1]. It is sufficient to use a constant value of 160 J/g. With bitumen, the melting enthalpy is larger. In practice, a value of 200 J/g is has proven best. With crude oils and heavy oils, a value of 160 J/g is recommended below 30 °C and a value of 200 J/g above 30 °C.
For a number of practical reasons, the problems mentioned at the beginning in connection with crystals separating out on cooling are particularly important. With crude oils and heavy oils, it is best to measure the crystallization in the temperature range 80 °C to -20 °C at a cooling rate of 2 K/min; and with medium heavy fuel oils, between 25 °C to -30 °C at a cooling rate of 0.5 K/min. In such experiments, a more or less pronounced exothermic peak is observed that shows the course of the crystallization. For the evaluation of the corresponding DSC curve, one distinguishes between the following characteristic temperatures:

- the turbidity (cloud) point, with crude and heavy oils often also called the wax appearance temperature (WAT), corresponds to the temperature at which crystallization begins (ASTM D2500).
- the CFPP, Cold Filter Plugging Point, corresponds to the temperature below which all crystallizable material has crystallized (EN 116).
- the flow point (FP) is the temperature at which the viscosity of the sample is so high that it no longer flows (ASTM D97).

To evaluate the crystallization peak, a horizontal or tangential baseline is drawn on the left side of the curve. A value of 200 J/g is assumed for the crystallization enthalpy.

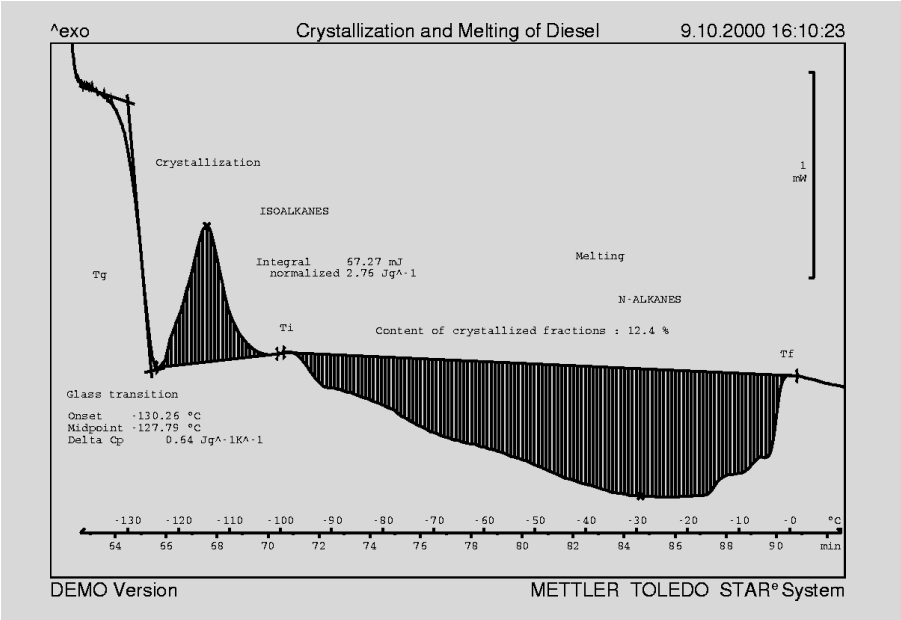

Fig. 2. Evaluation of a DSC curve of diesel oil

Evaluation of DSC curves of petroleum products

The crystalline components are embedded in the liquid matrix. The matrix is characterized by the glass transition temperature T_g and the step height of the change of the specific heat. The glass transition temperature correlates well with the average mole mass of the matrix. The percentage amount of the crystallized fractions can be calculated by dividing the measured heat of fusion by the (in principle temperature-dependent) melting enthalpy $\Delta H(T)$ of a fictive, fully crystallized sample.
For the compounds considered here, a linear baseline can be used for the determination of the peak area. This begins at about T_g +30 K (T_i) and ends at about 10 K after the end of the melting process (T_f). The melting enthalpy of the crystallized material can be estimated in the following way.

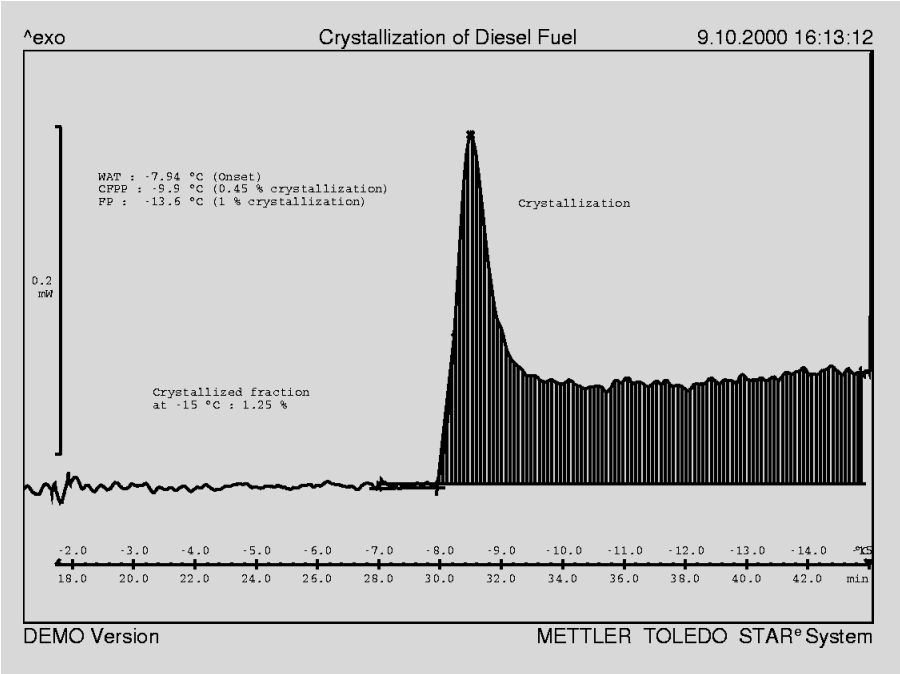

Fig. 3. Typical crystallization behavior of diesel oil

Example 1: light petroleum distillate (Fig. 3)

The turbidity point is taken to be the onset temperature of the crystallization peak (T_{onset}). The turbidity point defined in this way can be reproducibly measured with an accuracy of ±0.5 K. The values obtained with this method are slightly lower than those determined using the ASTM standard method (T_{ASTM}). The measurement of 50 different light distillates led to the following correlation:

$$WAT = T_{onset} = 0.98 \cdot T_{ASTM} - 3.6$$

For the determination of the CFPP value, the analysis of 40 light petroleum products gave the following correlation between the temperature at which 0.45% of the crystallizable material has crystallized out ($T_c(0.45\%)$) and the CFPP determined according to EN 116:

$$T_c(0.45\%) = 1.01 \cdot T_{CFPP\ EN\ 106} - 0.85.$$

For the determination of the flow point we found the optimum correlation to be:

$$T_c(1\%) = 1.02 \cdot T_{flow\ point\ ASTM} - 0.28$$

[2]. Here, $T_c(1\%)$ is the temperature at which 1% of the crystallizable fractions has crystallized out.

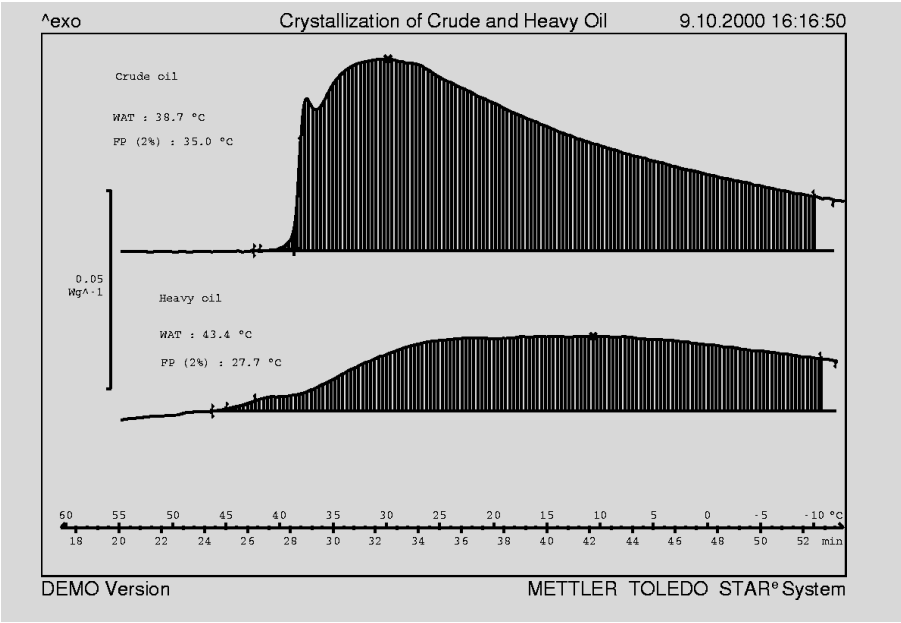

Fig. 4. Typical crystallization behavior of diesel oil

Example 2: heavy and crude oils (Fig. 4)

The determination of the turbidity point for heavy and crude oils is performed in a similar way to the light petroleum products. If the flow point is below 0 °C, the crystalline content after cooling is only about 2 mass%. The behavior of the sample is therefore for the most part determined by the noncrystalline matrix [3].

Conclusions

DSC measurements allow a rapid and reliable characterization of extremely different types of petroleum products. The glass transition temperature and melting behavior provide important information on the quality of petroleum derivatives. In addition, the origin of a sample of unknown petroleum can be determined because the measured curves are characteristic of the petroleum, i.e. they are "fingerprints". Cooling experiments yield important practical information on the crystallization behavior of petroleum derivatives.

Literature

[1] *F. Bosselet, Thèse Saint Etienne n°008 (1984)*

[2] *P. Claudy, J.M. Létoffé, B. Neff, B. Damin, FUEL, 65 (1986) 861-864*

[3] *J.M. Létoffé, P. Claudy, M.V. Kok, M. Garcin, J.L. Volle, FUEL, 74 (6) (1995) 810-817*

Applications of Differential Scanning Calorimetry to thermosetting materials

Dr. B. Benzler, Applikationslabor Mettler-Toledo, Giessen

Introduction

Differential Scanning Calorimetry (DSC) allows endothermic or exothermic enthalpy changes in a sample to be quantitatively measured. Melting processes in partially crystalline plastics, glass transitions and chemical reactions such as the curing of thermosetting resins can all be routinely analyzed [1].

The heat capacity increases on heating above the glass transition. The glass transition temperature, T_g, and the change of the specific heat capacity at the transition, Δc_p, are characteristic of the state of a plastic. If intramolecular and intermolecular mobility become restricted, for example as a result of increased crosslinking, then the glass transition temperature increases. Δc_p allows certain conclusions to be drawn about molecular interactions.

Prepregs are semi-finished products made from fabric impregnated with resin hardener mixtures. They are used to manufacture thermosetting molded materials through the action of pressure and temperature [2]. During the course of the development of a resin system for SMC prepregs (Sheet Molding Compounds) on the basis of unsaturated polyester resins (UP resins), the following questions arose concerning:

- the control of reactivity, e.g. whether the desired degree of cure is achieved even if the formulation is varied,
- the optimum duration of the compression (i.e. molding) and curing operations, and
- how long the prepregs can be stored, i.e. their storage stability.

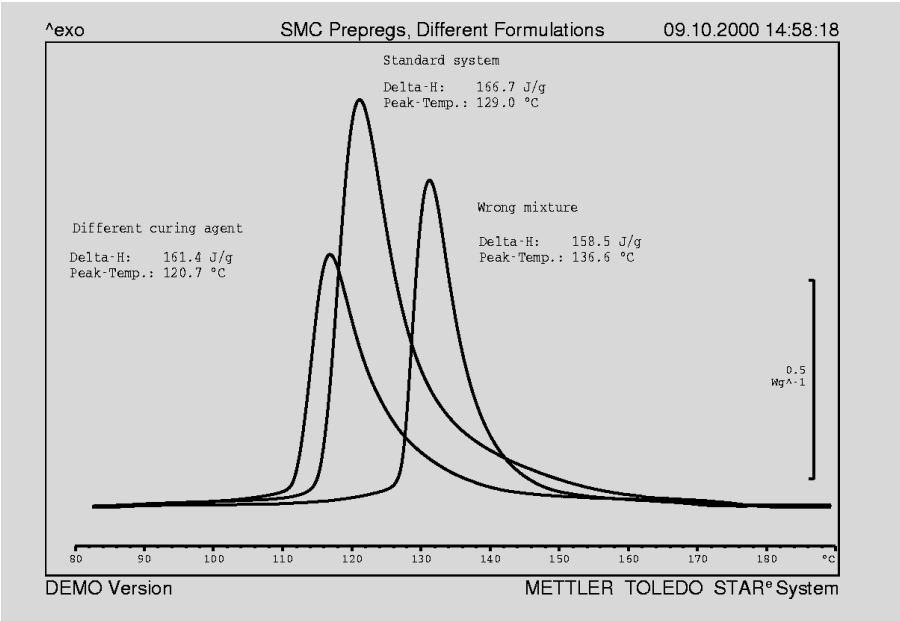

Fig. 1. DSC curves of different formulations measured at a heating rate of 3 K/min. Samples of 50 to 70 mg prepreg were weighed into the medium pressure crucible. Besides the usual formulation ("Standard system"), a formulation with a different hardener ("Different curing agent"), and a formulation in which one of the constituents had been left out ("Wrong mixture") were measured.

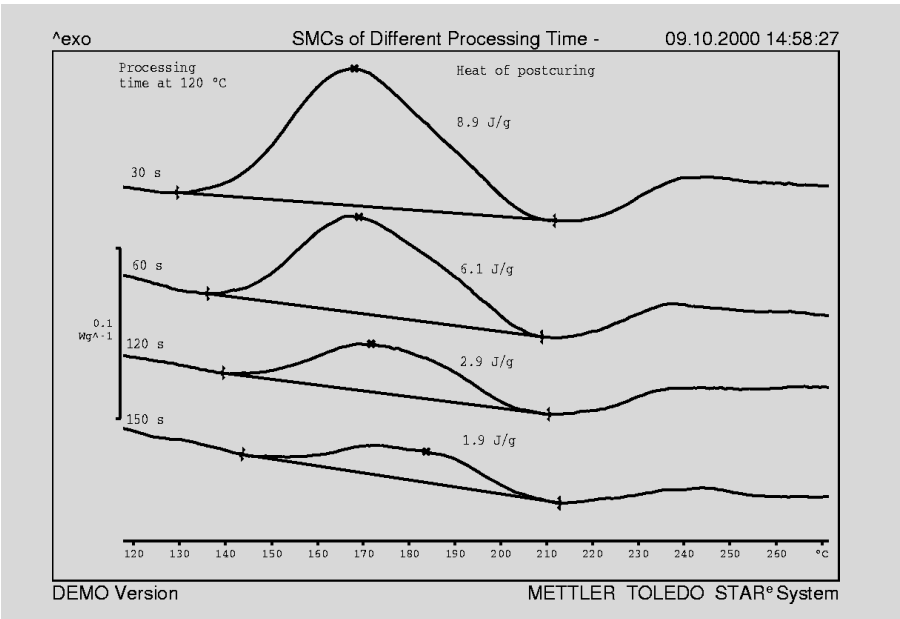

Fig. 2. With increasing curing time at 120 °C, the glass temperature increases while at the same time the heat of the postcuring reaction decreases. The heating rate used was 20 K/min.

Investigating the reactivity, keeping to the formulation

Figure 1 shows the DSC curves of three different resin/hardener formulations. The curing reaction is observed as an exothermic peak. The value Delta H (ΔH) corresponds to the normalized peak area in joules per gram of sample and therefore to the heat of reaction.

For a resin/hardener system, the larger the heat of reaction, the higher the degree of cure of the material. The standard formulation ("Standard system") contains the resin and hardener (curing agent) in a ratio that had proven to be good empirically. The temperature normally used for the simultaneous curing and molding process was 120 °C. The middle curve ("Standard system") shows the dynamic DSC curing reaction of a sample of this material measured at a heating rate of 3 K/min. On one occasion, when a curing agent was by mis-

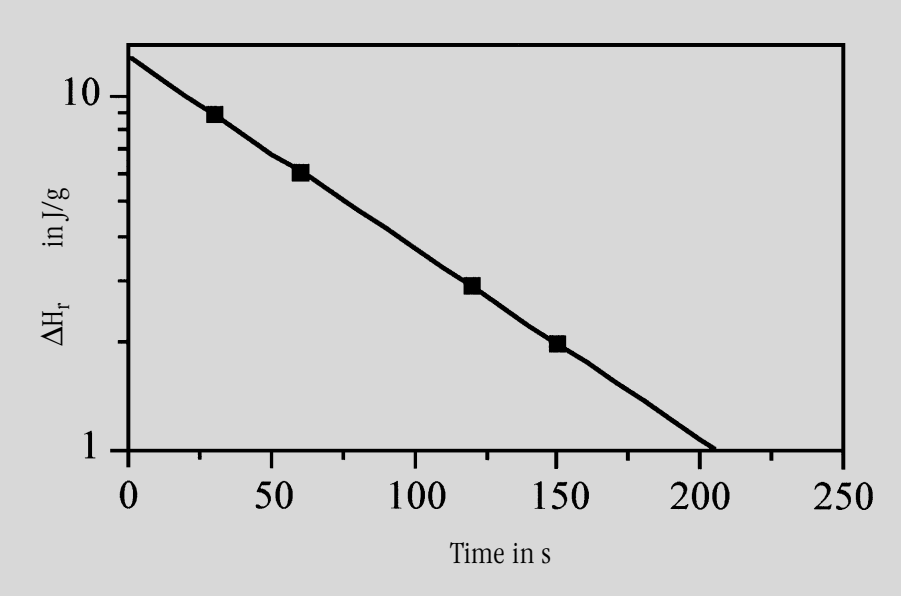

Fig. 3. The heat of postcuring (logarithmic) measured by DSC as a function of molding time.

take omitted, a faulty batch ("Wrong mixture") was produced. The curing reaction of this material took place at a significantly higher temperature, and the heat of reaction was noticeably smaller. This means that curing at the usual processing temperature (i.e. 120 °C) would either not be possible or would at best be very unsatisfactory. The third curve ("Different curing agent") is a formulation with a different hardener.

Investigation of the influence of molding time

Molding and curing of this SMC prepreg is done at 120 °C under pressure in a molding press. DSC can also determine the time required for this process. To do this, a number of test plates of the same composition were subjected to different molding times. The postcuring reaction of each of the plates was then investigated with DSC. The resulting curves are shown in Figure 2. The glass temperature increases during the course of curing. At the same time, the step height at the transition decreases, which is typical for these UP resins. The postcuring reaction gives rise to exothermic peaks that become successively smaller because the degree of cure increases with increasing molding time. The relationship between the enthalpy change of the postcuring reaction ΔH_r and the molding time is given by the following equation:

$$\ln \Delta(H_r) = a - b \cdot t$$

For a first order reaction, "a" is equal to the logarithm of the heat of reaction and "b" is equal to the rate constant of the curing reaction at the molding temperature. From Figure 3 it can be seen that no further significant postcuring takes place (< 1 J/g) when the molding time is 210 s or longer, i.e. the resin is effectively cured (e^a = 12.9 and b = 0.0054 s^{-1}).

In Fig. 1 (heating rate 3 K/min) the DSC curve of the curing reaction begins to deviate from the baseline at about 100 °C. A correspondingly slower reaction is however expected at lower temperatures. In particular, the reaction proceeds slowly even at room temperature, which makes prepregs unusable after a certain storage time. To investigate the storage stability, several prepregs were stored for different periods of time at 30 °C and then measured with DSC at 10 K/min. The results are summarized in Figure 4. The positions of the peaks on the temperature axis do not differ to any great extent. However, it is clear that the heat of the curing reaction decreases with increasing storage time. Experience shows that a degree of cure of up to about 30% can be tolerated. The storage time of this prepreg should therefore not exceed 6 days at 30 °C.

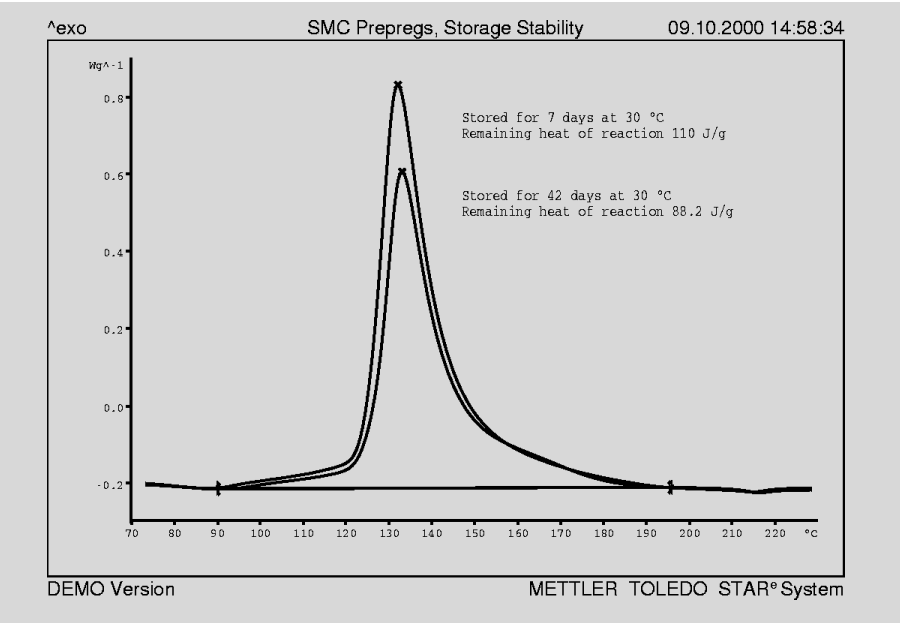

Fig. 4. After storing for 7 days at 30 °C, the remaining heat of reaction decreases from the initial value of 167 J/g to 110 J/g, and after 42 days to just 88 J/g. These DSC curves were measured at 10 K/min.

Conclusions

These practical examples show that simple investigations with Differential Scanning Calorimetry provide an enormous amount of information and allow many questions of a practical nature to be answered. Apart from establishing, optimizing and checking the formulation, the molding time for the curing and molding process and the storage stability of the prepregs can also be determined. The main experimental quantities used for the evaluation are the exothermic heats of the curing and postcuring reactions. The glass transition temperature also yields useful additional information.

Literature

[1] *B. Benzler: Dynamische Differenzkalorimetrie - Hohe Reproduzierbarkeit Plastverarbeiter 47 (1996) 9, Seite 66*

[2] *B. Benzler: Vollständig vernetzt ? Dynamische Differenzkalorimetrie an EP-Harzen Plastverarbeiter 47 (1996) 11, Seite 58*

Force and temperature modulated TMA measurements of fibers

Dr. R. Riesen

Intruduction

Thermal shrinkage is an important property of fibers that depends on the structure of the individual fibers concerned and on the processing conditions used, i.e. thermal history [1]. Shrinkage can be measured by classical Thermomechanical Analysis (TMA) using a low tensile force (load) at constant heating rate. The linear coefficient of expansion α_e of a sample that does not shrink can be determined in the same way. Young's modulus (E) can also be measured with TMA by modulating the tensile force during the heating program [2].

With drawn (stretched) fibers, however, the expansion that occurs on heating is superimposed on the shrinkage and cannot therefore be measured directly by TMA. Expansion and shrinkage are processes that are physically linked via the structure of the sample. When structural relaxation occurs, both properties change, but at different rates, because they are controlled by different effects (e.g. free volume and crystal perfection). In addition, shrinkage is influenced by irreversible changes in the internal stress. As a result of this, α_e changes on shrinking, and the original thermal expansion coefficient of a stretched fiber cannot therefore be determined in a second heating measurement.

A special technique, known as temperature modulated TMA, is used to simultaneously determine expansion and shrinkage behavior. In much the same way as temperature modulated DSC (ADSC), a modulated heating rate is superimposed on the mean heating rate. As a result of this, the temperature oscillates sinusoidally, e.g. it oscillates up and down every three minutes with a maximum of 5 K/min and a minimum of -4 K/min at a mean rate of 1 K/min. The sample shrinks slowly and irreversibly due to the increase of the mean temperature. The normal reversible expansion, however, follows the small temperature changes.

This means that α_e can be determined from the oscillating changes in length induced by the temperature modulation independent of the shrinkage coefficient α_s [3].

Young's modulus (E) is determined from the change in length that occurs when the tensile force is modulated. If the frequency of this modulation is appreciably higher than that of the temperature modulation, then both excitations can be applied simultaneously. Fourier analysis is then used to calculate E, α_e and α_s from the TMA measurement curve.

Basic equations

Coefficients of linear expansion and shrinkage

When a stretched fiber is heated, structural changes cause large changes in length. The apparent coefficient of expansion α_e^* is determined from the measurements according to equation 1:

$$\alpha_e^* = (dL/dT) / L_0 = \nu / (\beta \cdot L_0) \qquad (1)$$

L: length, T: temperature,
L_0: original sample length, t: time,
$\nu = dL/dt$ the rate of change of length,
$\beta = dT/dt$ the heating rate.

The measured apparent expansion of fibers on heating can be separated into a reversible and an irreversible part, i.e. the apparent expansion is the sum of the actual thermal expansion and the shrinkage:

$$\alpha_{e^*} = \alpha_e + \alpha_s \qquad (2)$$

α_e: thermal coefficient of expansion
α_s: coefficient of shrinkage

The relaxation process on shrinking is normally slow and predominantly time-controlled. The thermal expansion, however, follows the temperature modulation. The rate of change of length can therefore be considered as being made up of two parts:

$$\nu = (\alpha_e^* \cdot \beta_{mean} + \alpha_e \cdot \beta) \cdot L_0 \qquad (3)$$

β_{mean}: mean heating rate

Analogous to equation 1, α_e can be determined from the amplitude of the rate of change of length ν_A and the amplitude of the instantaneous heating rate β_A:

$$\alpha_e = \nu_A / (\beta_A \cdot L_0) \qquad (4)$$

The amplitude ν_A is determined from the measured ν-curve using Fourier analysis. If the sample temperature follows the superimposed modulation, then β_A is equal to the programmed amplitude. If this is not the case, e.g. at low temperatures, then the heating rate and its amplitude can again be calculated by Fourier analysis from the sample temperature, which is measured very close to the fiber.
The apparent coefficient of expansion α_e^* is calculated from the mean values of ν_{mean} and β_{mean} obtained by Fourier analysis according to equation 5:

$$\alpha_e^* = \nu_{mean} / (\beta_{mean} \cdot L_0) \qquad (5)$$

The coefficient of shrinkage α_s is the difference between the apparent coefficient of expansion and the effective thermal coefficient α_e (equation 2).

Young's modulus

Young's modulus is determined from the ratio of the applied tensile stress and the expansion (equation 6). Young's modulus can also be measured during shrinking from the modulation of the tensile stress on heating.

$$E = (\Delta F/A) / (\Delta L/L_0) \qquad (6)$$

where ΔF is the change of the tensile force (load change in the TMA experiment), A is the cross-sectional area of the fiber, ΔL is the corresponding change in length, and L_0 the length of the fiber.

It is assumed that ΔL is very small in com-

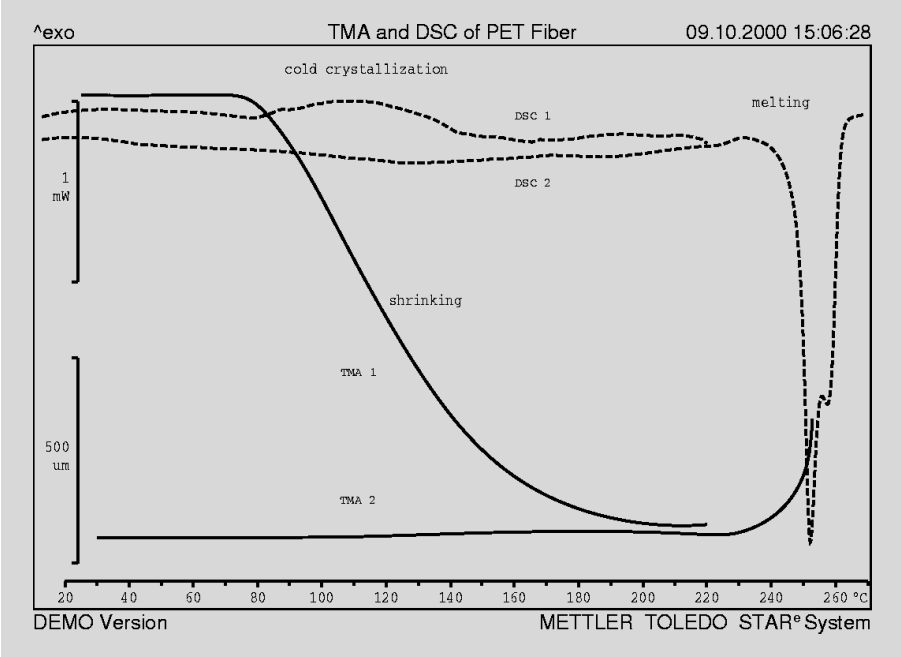

Fig 1. Conventional TMA and DSC curves of a PET fiber. First heating run up to 220 °C (1) and a second heating run up to 270 °C (2) with nonprogrammed cooling in between. DSC: 2.51 mg fiber in a 20 µl aluminum pan; TMA: 13 mm fiber with a tensile load of 0.1 N. Purge gas: nitrogen, 50 ml/min. Heating rate: 10 K/min.
DSC: exothermal direction upward; TMA: expansion direction upward.

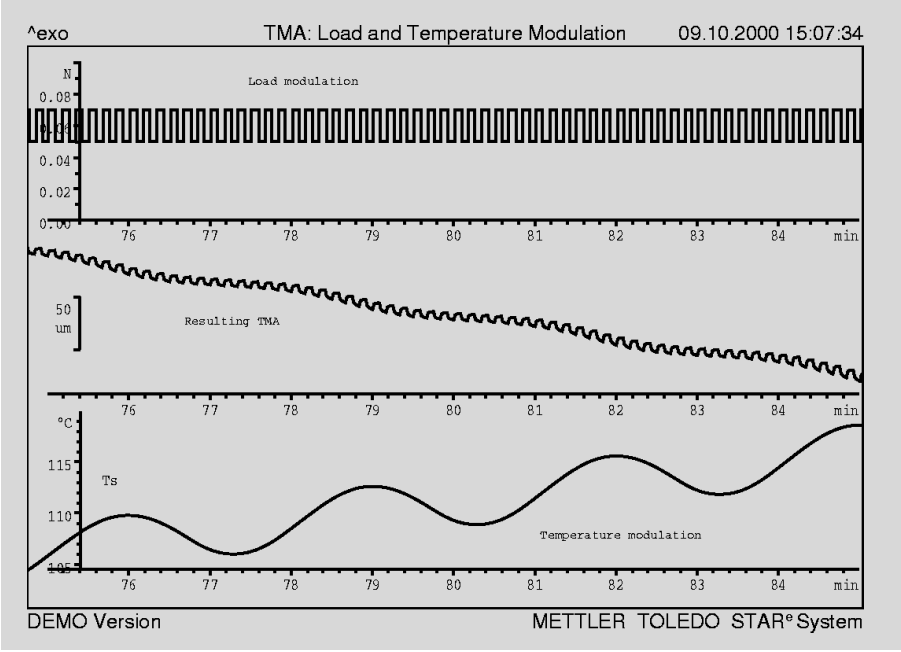

Fig. 2. TMA curve of the PET fiber with load and temperature modulation during the first heating run. The range 105 °C to 115 °C is shown expanded to demonstrate the effect of modulation more clearly.

parison to the length of the fiber. ΔL is once again determined from the TMA curve by Fourier analysis.

Experimental

The measurements were performed using a METTLER TOLEDO STARe System consisting of a TMA/SDTA840, DSC821e and all the necessary software options (ADSC for Fourier analysis, TMA for modulus calculations and Math Evaluation for the division of curves). The measurements were performed on polyethylene terephthalate fibers (PET, Viscosuisse type 260, 108 dtex, 0.10 mm diameter) that were mounted in the sample holder using copper clips so that the length of the sample was initially 13 mm. In the evaluation, the expansion of the clips and the quartz glass sample holder is software-compensated. The temperature calibration and adjustment was performed as described in references [3] and [4]. The program used for the measurements was: heating from 30 °C to 230 °C at a mean rate of 1 K/min with a modulation amplitude of 2 K and a period 3 min. The load was square-wave modulated between 0.05 N and 0.07 N with a period of 10 s. The relatively large temperature modulation was necessary in order to be able to determine small coefficients of expansion accurately. If other conditions were used, it is referred to in the discussion of the results.

Results

The thermal behavior of the PET fiber under investigation is shown in the first and second TMA and DSC heating runs (Fig.1). Shrinking begins immediately after the glass transition at 79 °C and amounts to 8.1%. Cold crystallization also begins after the glass transition; the heat of crystallization measured by DSC was 13.8 J/g. The heat of fusion is 52.4 J/g. In the second heating run the actual expansion does not begin until about 106 °C, followed by slight shrinking shortly before melting begins. No further cold crystallization was observed.
In order to separate the effects of expansion and shrinkage, the PET fiber was measured in a temperature modulated TMA. Part of the measurement program is displayed in Figure 2. Force and temperature modulation can be clearly seen on the TMA curve. The fact that the TMA curve steadily slopes downward shows that shrinkage does not stop during the short cooling phases. The equilibrium condition would only be reached after a longer isothermal period at the particular temperature [3].
The changes in length caused by the load modulation (Fig. 2) were evaluated according to equation 6 and Young's modulus determined as a function of temperature. Figure 3 shows the TMA curves and Young's modulus for the first and second heating runs.
After the first heating run, the sample relaxes and the crystals are perfected. The values of Young's modulus for the stretched (original) and relaxed fibers are about the same, but the temperature dependence is

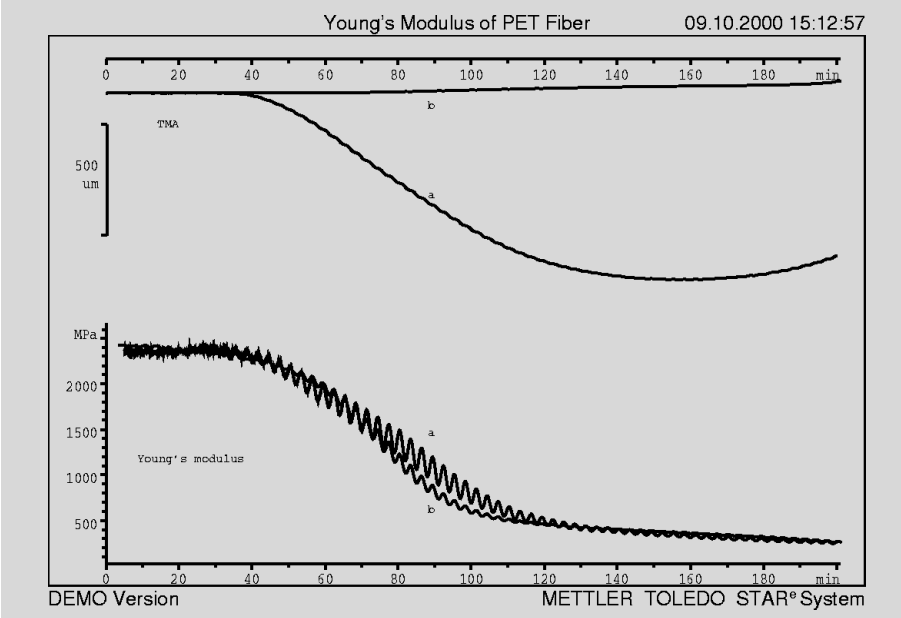

Fig. 3. TMA curves of the PET fiber (mean of the load-modulated curves shown in Fig. 2). Young's modulus curves were calculated by Fourier analysis from the load-modulated TMA curves and are shown as a function of time in the same temperature range as TMA curves. a: first heating run, b: second heating run of the same sample.

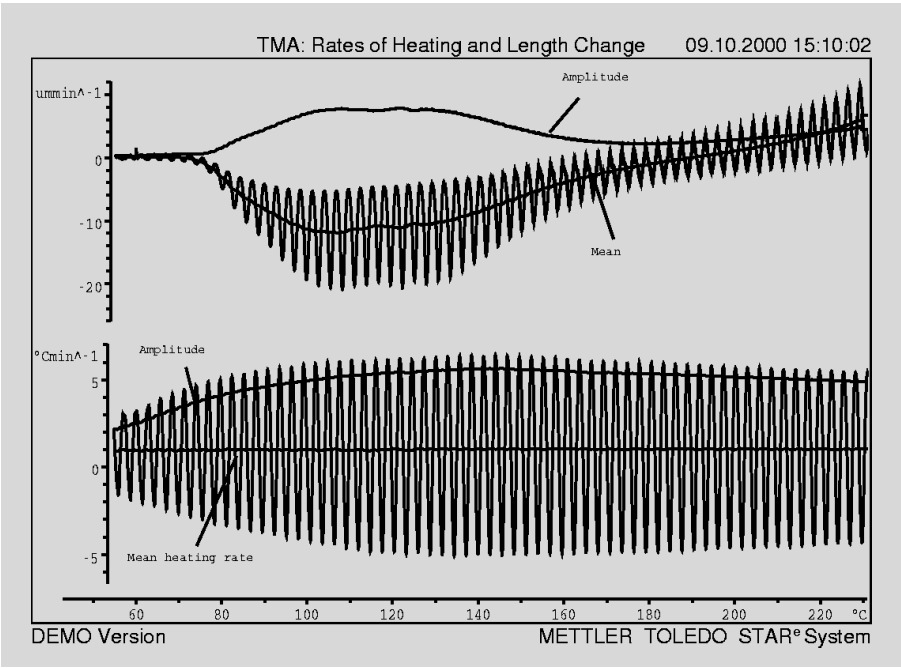

Fig. 4. Lower diagram: derivative of the sample temperature of the PET fiber during the first heating run. Upper diagram: derivative of the TMA curve ν with the load modulation filtered out. The corresponding mean curves (β_{mean}, ν_{mean}) and amplitude curves (β_A, ν_A) are calculated. The original TMA curve is shown in Figure 3. The temperature calculated from the mean heating rate was used as the abscissa unit.

however more pronounced during shrinkage than in the second heating run. Due to the remaining amorphous parts, a glass transition occurs in the fiber. In the region of the glass transition, Young's modulus follows the temperature modulation with a relatively large amplitude, but afterward the mean value decreases significantly. The derivative of the sample temperature (β as well as β_{mean}, and β_A) and the derivative of the corresponding TMA curve (ν as well as (mean and νA) are shown in Figure 4. These curves form the basis for the calculation of the coefficients of expansion and shrinkage according to equations (4), (5) and (2).

The coefficient of expansion α_e was calculated from the amplitude according to equation 4 and the apparent coefficient of expansion α_e* from the mean values (equation 5). Figure 5 shows the resulting curves as a function of temperature for the first and second heating runs of the same fiber.

Figure 6 shows the corresponding coefficients of shrinkage ($\alpha_s = \alpha_e^* - \alpha_e$) calculated from the curves in Figure 5.

In the first heating run, shrinkage predom inates. Nevertheless, α_e increases due to the increase in the free volume of the amorphous part. Two processes contribute to this: the glass transition and an additional structural relaxation. Above 100 °C, cold crystallization begins (see Fig.1), which reduces the amorphous part and thereby reduces the coefficient of expansion. At higher temperatures, the fiber recrystallizes, leading to a further change in α_e. The first heating run was stopped at 230 °C, i.e. at a temperature well below the melting temperature. This allowed the sample to be used for the second measurement.

At the beginning of the second heating run, α_e is very small, but increases in the region of the glass transition. Above 210 °C, crystals formed after the first heating run begin to melt. This affects α_e. In this connection, it should be mentioned that α_e always refers to the coefficient along the length (i.e. in the direction) of the fiber and does not take changes in the total volume into account.

Comparison of the values of α_e from modulated and unmodulated TMA measurements (the second heating runs, Fig. 1 and 5) shows practically the same behavior in both cases; at 50 °C both coefficients are very small and the values increase to $20 \cdot 10^{-6}$ °C^{-1} at 130 °C.

Since no shrinkage occurs in the second heating run, it is to be expected that the values of α_e* and α_e are the same. As can be seen in Figure 5, this is true within the limits of measurement accuracy up to the temperature at which PET begins to flow (above 210 °C).

The coefficient of shrinkage α_s (Fig. 6) shows irreversible contraction beginning at the glass transition. Near the melting range, this coefficient becomes positive and shows the irreversible stretching of the fiber due to the sample beginning to flow.

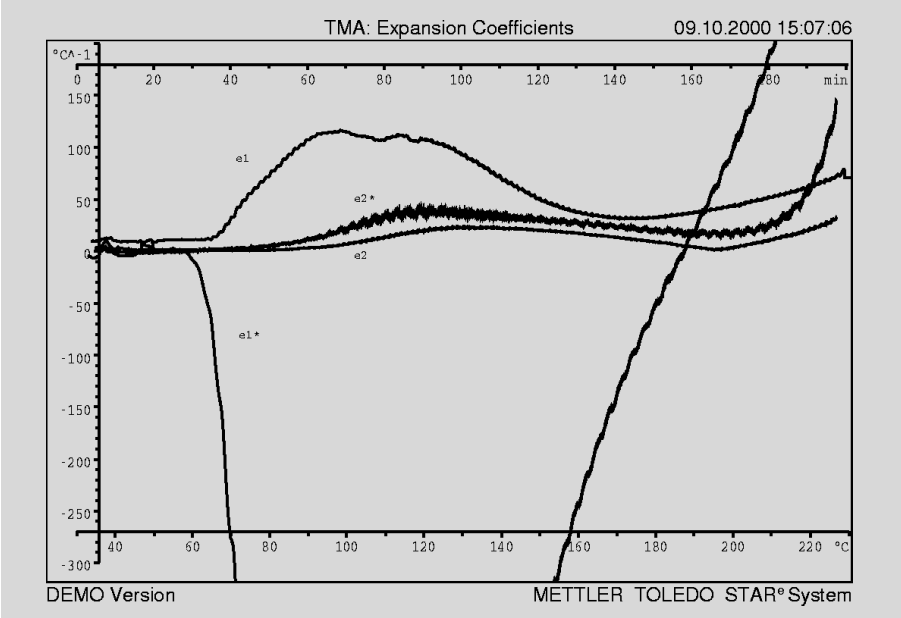

Fig. 5. Coefficients of expansion of a PET fiber calculated from the curves in Figure 4; the numbers 1 and 2 refer to the first and second heating runs. The ordinate scale is given in units of $°C^{-1}$, the coefficients α_e and α_e* (e, and e*) should be read in units of µm/(m °C).

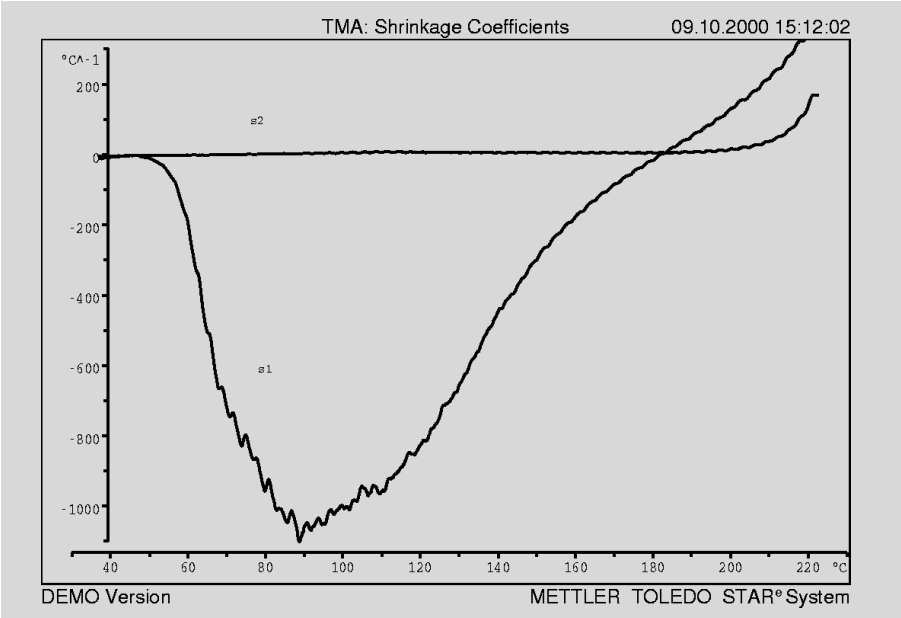

Fig. 6. Coefficient of shrinkage α_s for the first (s1) and the second (s2) heating runs of the PET fiber, calculated from the curves in Figure 5. The ordinate scale is in units of $°C^{-1}$, the coefficients α_s should be read in units of µm/(m °C).

Conclusions

With temperature-modulated TMA, it is possible to determine the thermal expansion and shrinkage of a drawn (stretched) fiber separately during the relaxation process. For reasons of heat transfer, only low frequencies can be used for temperature modulation. The tensile stress can therefore be simultaneously modulated at higher frequencies, allowing Young's modulus to be determined at the same time. These properties can also be determined as a function of temperature. One single, double-modulated TMA measurement therefore enables you to investigate three important properties and hence study the effect of stretching conditions and other manufacturing processes. The method presented can of course also be applied to similar processes with other materials (e.g. films) for penetration, expansion, bending and swelling measurements.

Literature

[1] *M. Jaffe, Thermal Characterization of Polymeric Materials, 2nd Edition, E.A. Turi Ed., Academic Press, New York 1997, 1767.*

[2] *H. G. Wiedemann, R. Riesen, A. Boller, ASTM STP 1136, American Society for Testing and Materials, Philadelphia (1991) 84.*

[3] *R. Riesen, J. E. K. Schawe, J Thermal Anal. 59 (2000) 337-350.*

[4] *Expansion and shrinkage*

Measurement of pore size distribution with DSC

Thad C. Maloney, Helsinki University of Technology, P.O. Box 6300, FIN-02015 HUT, Finland, e-mail: Thad.Maloney@hut.fi

Introduction

Pore size distribution (PSD) is a critical property of many materials. Ceramics, catalysts, pharmaceuticals, and the author's own special area of interest namely cellulosic pulp fibers, are examples of such materials. The classical methods for measuring pore size distribution are gas sorption and mercury porosimetry. An interesting alternative technique is based on DSC and is commonly known as thermoporosimetry. In this article, thermoporosimetry refers to the measurement of pore size density based on the determination of the melting point depression of an absorbate held in a porous material. The relationship between the pore diameter (D) and the melting temperature depression (ΔT_m) is described by the well-known Gibbs-Thomson equation:

$$D = \frac{4\,V\,T\,\sigma_{ls}}{\Delta H_m\,\Delta T_m} \qquad (1)$$

where V is the molar volume, T the melting point of large crystals of the selected adsorbate, ΔH_m the heat of fusion, and σ_{ls} the surface energy at the liquid-solid interface. Although almost any substance can be used as the adsorbate, water is one of the most attractive substances to fill the pores, because the melting point lies in a temperature range that can easily be measured. For water, V = 19.6 10^{-6} m^3/mol, T = 273.14 K, ΔH_m = 6.02 kJ/mol. The value of σ_{ls} was determined by measuring the melting point depression of water in a series of controlled porous glass (CPG) standards of known pore diameter by DSC. The result obtained from these measurements was 12.1 mN/m. The relationship between pore size and melting point depression is therefore:

$$D = 40.3\ \text{nm K} / \Delta T_m \qquad (2)$$

A basic problem in thermoporosimetry is that the equilibrium melting temperature T_m must be determined as accurately as possible in order to calculate the difference ΔT_m between it and the melting point T. In fact, even slow heating rates can give rise to temperature gradients that affect the results. One way to overcome this problem is to use a temperature program with isothermal steps in the melting range. The temperature is held constant until the sample and reference temperatures are in equilibrium with the furnace temperature, i.e. $T_s \approx T_r \approx T_c$. An isothermal step program is shown schematically in Figure 1. Three parameters are required to define such a temperature program:

1. The duration of the isothermal segment Δt_{iso} must be long enough for melting to reach an equilibrium state.
2. The temperature step, ΔT, determines the resolution of the measurement. Materials with a narrow pore size distribution need a correspondingly small ΔT.
3. The heating rate, β, of the dynamic segment between two steps should be sufficiently slow to avoid large fluctuations of the DSC signal as the DSC switches from the heating mode to the isothermal mode and vice versa, but fast enough to facilitate a rapid measurement. The optimum parameters are sample dependent.

One important advantage of the isothermal step method is that it allows very small melting temperature depressions to be accurately measured. This, however, requires extremely high temperature stability in this step mode type of operation. The value for the DSC 821^e is about 0.02 K. This enables pores sizes of up to about 430 nm to be measured.

The total volume V of the pores with the relevant diameter for an isothermal step can be determined from the peak area (heat of fusion H_l) measured at this temperature by the equation:

$$V = H_l / (\rho \cdot 334.5\ \text{J/g}) \qquad (3)$$

where ρ is the density of the water at the corresponding temperature, and 334.5 J/g is the specific heat of fusion of water.

In this case, the temperature dependence of the heat of fusion and the heat capacity is neglected.

ΔT_m/K	40	20	10	5	2	1	0.5	0.2	0.1	0.05
D/nm	1	2	4	8	20	40	80	200	400	800

Table 1. Melting point depression and pore size

Experimental

The measurements were performed with a DSC821^e equipped with an IntraCooler. The purge gas was nitrogen at 50 ml/min. The results were evaluated with the STAR^e software package.

For thermoporosimetry, accurate temperature calibration in the range around 0 °C is essential. A two-point calibration with mercury and water gives good results and is recommended. The pan used for mercury should be treated beforehand to prevent the mercury reacting with the aluminum to form an amalgam (and thereby possibly making a hole in the pan). The treatment consists of subjecting the pan to water vapor in an autoclave at about 120 °C for several minutes, or by storing the pan for several days at 25 °C in air at 95% relative humidity, e.g. in a desiccator over water. Under these conditions, an inert film of aluminum hydroxide-oxide is formed on the surface of the pan.

The following isothermal step method was used for temperature calibration: Δt_{iso} = 5 min, ΔT = 0.02 K and β = 0.05 K/min. The melting point is taken to be the temperature at which the entire sample has melted. The temperature calibration obtained in this way is slightly different from that based on dynamic measurements.

Although tau lag is not important for the isothermal steps, it does have an effect on the dynamic segments in the measurement program. It was therefore adjusted in the usual way at various heating rates using the onset temperatures of the melting peaks of mercury and water. Heat flow calibration is performed on the melting peak of ice at 5 K/min. (NB Water can supercool to a marked degree; it does not usually crystallize until below -15 °C). Experiments performed beforehand showed good agreement between the peak areas of the isothermal and dynamic measurements. This means that dynamic calibration can be used for the isothermal step method.

For the determination of pore size distribution, water-saturated samples of 2 mg to 4 mg were hermetically sealed in standard 40 µl aluminum pans. The water must be present in excess, i.e. more than to just fill the pores. The sample used to determine the pore size should be washed well with pure water to avoid any additional melting point depression through the presence of impurities.

Measurements

The sample is first measured dynamically at a relatively slow heating rate (5 K/min) to determine the parameters for the step program. If the pores are sufficiently small, two peaks are obtained, one for the pore water and the other for the bulk (excess) water. Samples with large pores give rise to peaks that overlap (Fig. 2). If the maximum pore diameter is less than 100-200 nm, the step method can separate the peaks. If the samples have larger pores, a partial pore size distribution can still be obtained up to about 430 nm. This corresponds to a ΔT_m of 0.1 K.

The total water content of the sample is determined by drying after the experiment. The proportion of freezable pore water and the excess water is calculated from the corresponding peak areas by integration and division by 334.5 mJ/mg (equation 3). Adsorbed water does not freeze; the proportion can be obtained by subtracting the calculated freezable water from the total water.

The following parameters were used for the measurement of silica gel with isothermal steps (Fig. 3): Δt_{iso} = 5 min, ΔT = 0.3 °C and β = 0.5 K/min.

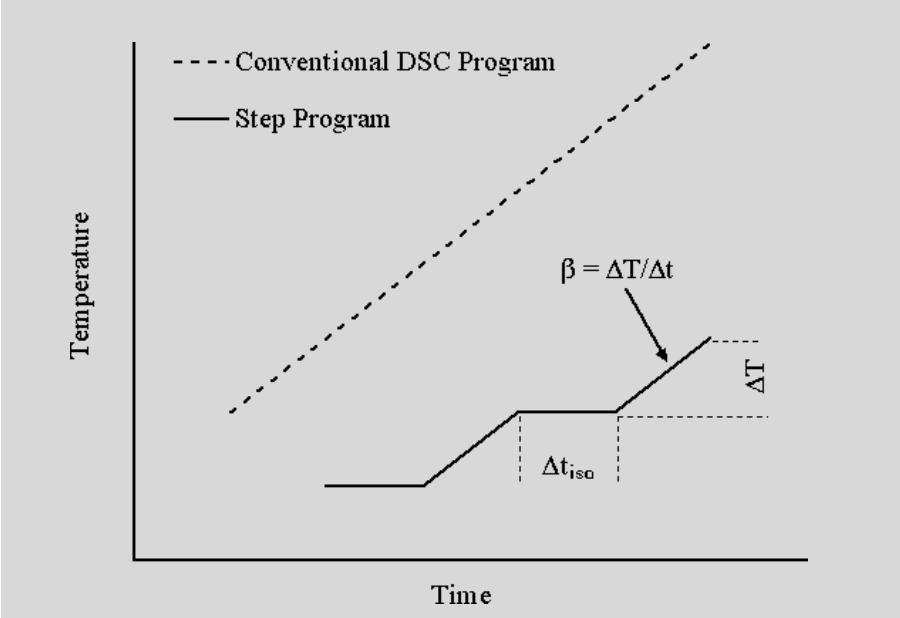

Fig. 1. Conventional DSC temperature program (dashed line) and an isothermal step program with the relevant parameters indicated.

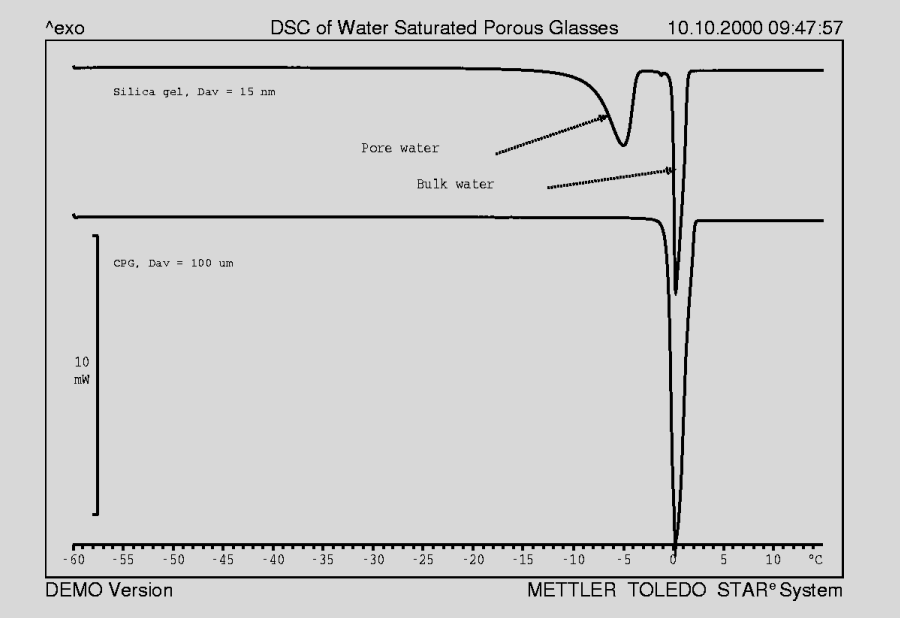

Fig. 2. Dynamic DSC curves of water-saturated porous glasses with average pore sizes (Dav) of 15 nm and 100 nm. β = 5 K/min. With a pore size of 15 nm, two melting peaks are observed - that of the pore water and that of the free (bulk) water.

Evaluation

1. Draw a baseline across the isothermal segment from the left to the right of the melting peak.
2. Subtract the baseline from the measurement curve. The curve corrected in this way now begins at zero (see Fig. 3, upper diagram).
3. Calculate the integral of the step curve (see Fig. 3, lower diagram).
4. Draw in the line of the sensible heat, H_s, (tangent from the left in Fig. 3, lower diagram).
5. Subtract the line of the sensible heat from the integral to obtain the (latent) heat of melting (H_l).
6. Set up a table of values for heat of melting versus temperature.
7. Import the values or table into a spreadsheet program.

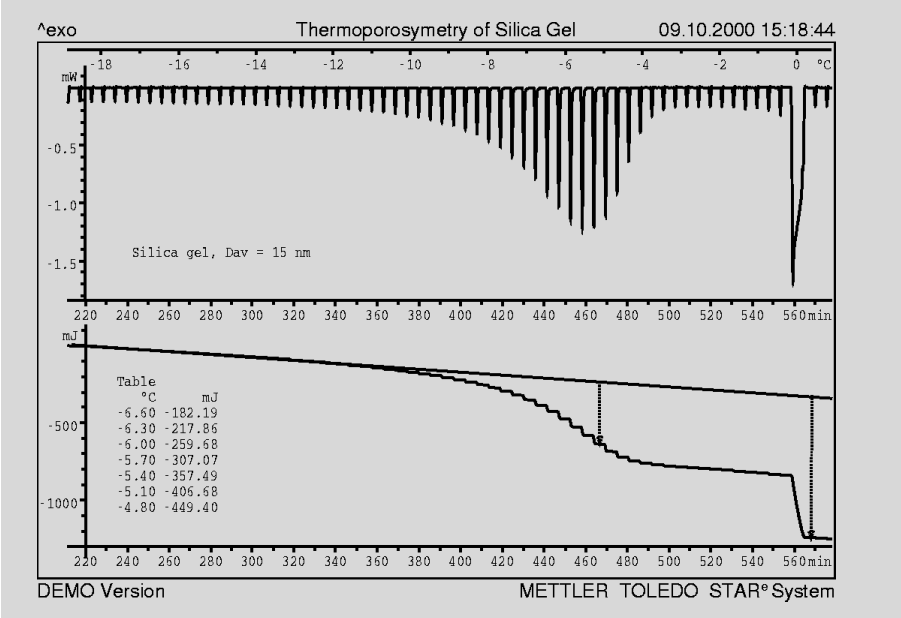

Fig. 3. Thermoporosimetry of a water-saturated porous glass. Upper diagram: isothermal step DSC measurement of a water-saturated porous glass with an average pore size (Dav) of 15 nm.
Lower diagram: result of the evaluation, points 1 to 4 (see text).

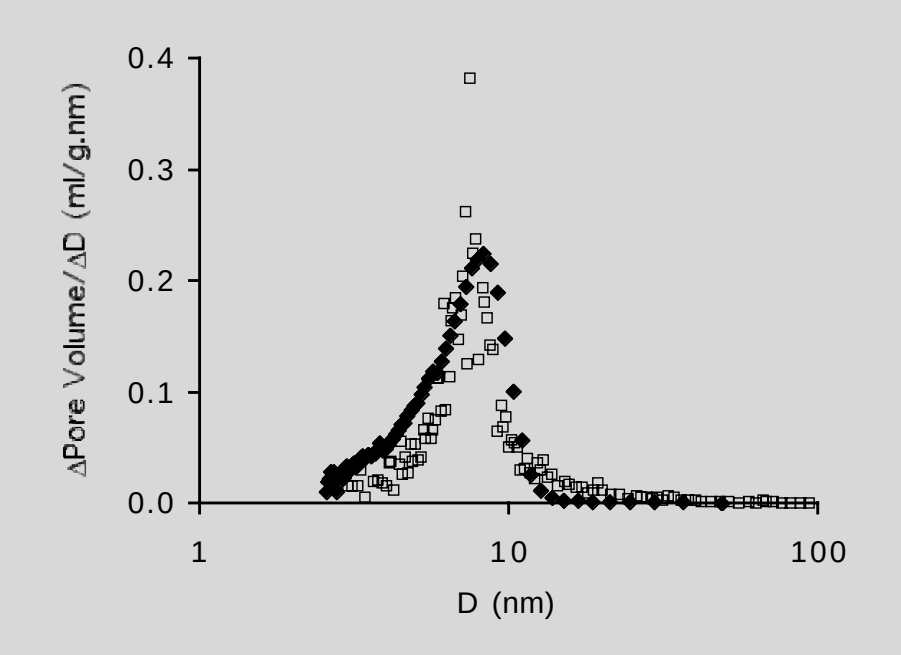

Fig. 4. The pore size distribution based on the measurement in Figure 3 (filled black squares). The results from mercury porosimetry (blank white squares) are presented for comparison purposes.

8. The amount of pore water and hence the pore volume is calculated from the heat of melting according to equation 3. The specific pore volume in ml/g up to the relevant pore size is obtained by dividing the pore volume by the dry mass of the porous sample (cumulative distribution).
9. The pore size follows from ΔT_m according to equation 2.
10. To obtain the pore size distribution, the difference between neighboring values of the cumulative distribution is divided by the difference of neighboring values of the pore size.

The pore size distribution of silica gel evaluated in this way agrees very well with the results obtained by mercury porosimetry (Fig. 4).
To reduce measurement time, it is sometimes advantageous to use a temperature program in which the size of the temperature step varies with temperature. Initially, at the beginning of the measurement, relatively large temperature steps are used. Smaller steps are then used where necessary in order to obtain better resolution (usually in the range of larger pores). This, however, complicates the evaluation of such nonequidistant isothermal step curves.

Conclusions

DSC isothermal step melting is a good way to determine pore size distribution. Temperature gradients are avoided and excellent temperature resolution is obtained. Pores with diameters of up to 430 nm can be determined with this method.
The measurement is easy to perform and is suitable for many different types of samples. The method can easily be optimized for maximum resolution or shortest measurement time by setting the size of the temperature increments accordingly.
DSC allows the measurement of moist samples, which is very advantageous for the investigation of hydrogels such as cellulose fibers. The pores of these materials exist only in the swollen state. By varying the water content, it is possible to observe how the pores disappear on drying. This type of measurement is not possible with gas sorption or mercury porosimetry because these methods require dry samples.

Measurement of low concentrations of PE-LD in PE-HD

Dr. M. Schubnell

Introduction

Small amounts of PE-LD are often added to PE-HD to modify its mechanical properties. The following experiments describe the use of DSC to determine the detection limit for such additions, and to investigate the extent to which these additions can be quantitatively determined in polymer mixtures. Four samples of different (known) PE-LD content were used for these experiments. The samples of pure PE were first measured. Figure 1 shows that the melting behavior of PE-LD differs clearly from that of PE-HD. Assuming at least a partial incompatibility of the two materials, one can expect the DSC melting curve of mixture of PE-LD and PE-HD to exhibit two clear melting peaks, as shown in Figure 1.

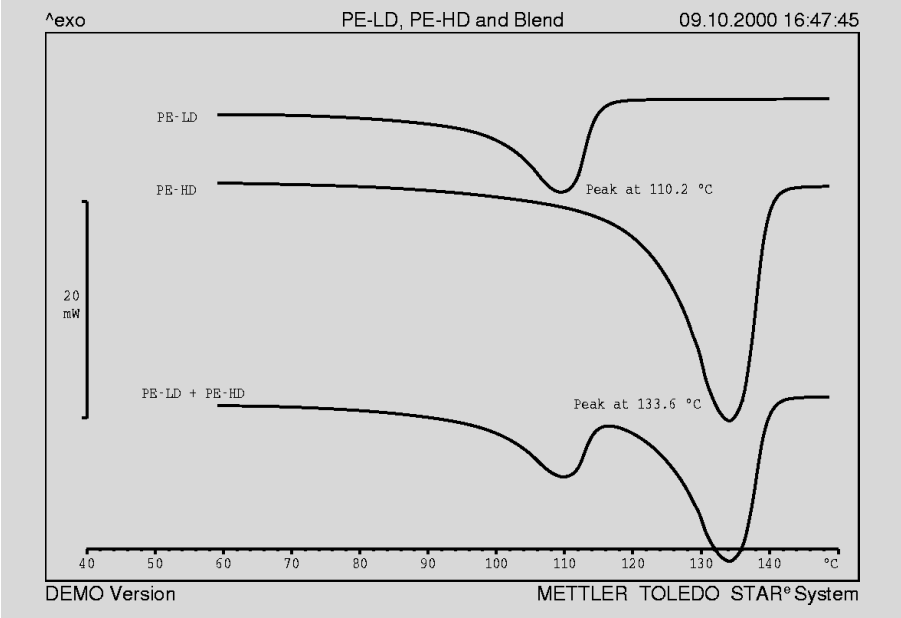

Fig. 1. Melting curves of PE-LD and PE-HD. The peak maximum of the PE-LD melting curve is appreciably lower. The crystallinity of PE-LD and PE-HD is also different; typically the degree of crystallinity of PE-HD is about 65%, and PE-LD about 25%.

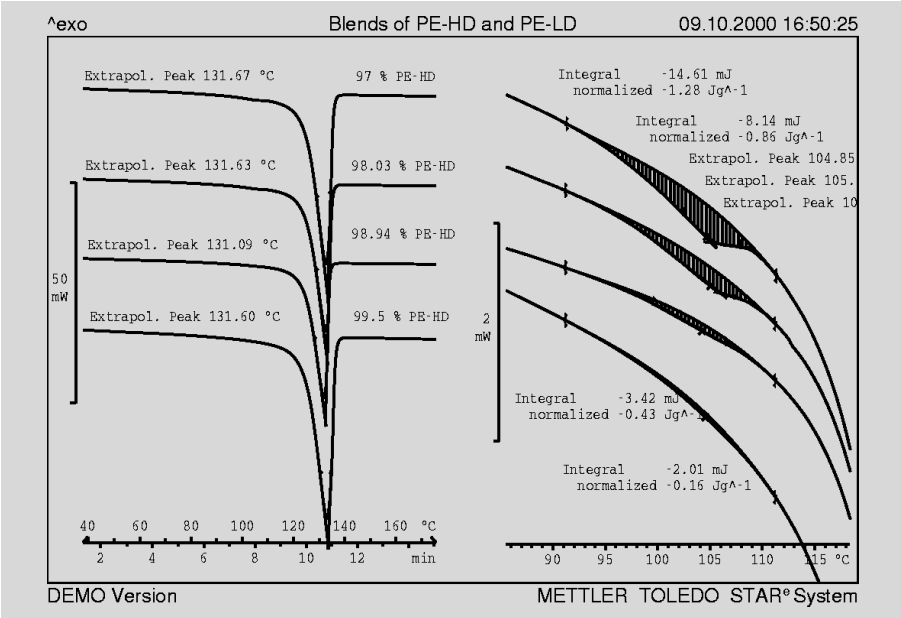

Fig. 2. DSC curves of mixtures of PE-HD/PE-LD of different PE-LD content. The curves on the right show sections of the curves from the left that have been greatly expanded

Experimental

Samples: PE-LD and PE-HD mixtures with PE-LD concentrations of 3%, 1.97%, 1.06% and 0.5%
Measuring cell: DSC821^e with IntraCooler
Sample preparation: pellets of about 10 mg in 20 µl aluminum pans
Heating rate: 10 K/min

Results

Figure 2 shows the DSC curves of the different samples. The broad melting peak of PE-HD of course predominates. The much smaller melting peak (shoulder) of PE-LD is superimposed on the low temperature side of PE-HD melting peak and is not very clearly defined because the PE-LD content of the samples is so low. Careful analysis of the PE-LD melting region shows that PE-LD concentrations of less than 1% can be clearly identified on the melting curve. The area of the superimposed PE-LD peak was integrated using the baseline type "Spline". The evaluation of the series of samples using identical parameters (such as baseline and temperature range) allowed an even smaller peak with a PE-LD content of 0.5% to be measured. The results show that the detection limit for PE-LD in a PE-HD matrix is about 0.5% PE-LD. The PE-LD content cannot of course be directly inferred from the peak areas. If the ratio of the partial areas to the total area is plotted as a function of the PE-LD content (see Fig. 3), then to a good approximation a straight line is obtained. In practice this means that the PE-LD content of an unknown sample can be estimated using a calibration measurement in which a sample of known PE-LD content is evaluated. This procedure of course assumes that the chemical structure (such as length and distribution of side chains) and physical structure (such

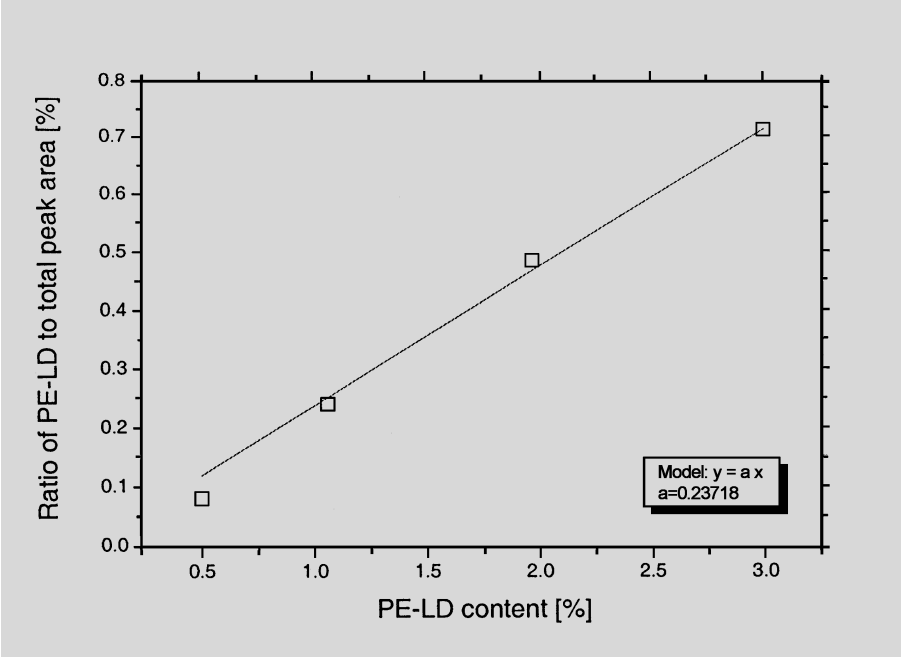

Fig. 3. Ratios of the PE-LD melting peak (baseline type Spline") to the total peak area as a function of the PE-LD content.

as degree of crystallinity) of all the components used and the preparation conditions (e.g. temperature and mixing technique) are identical.

Conclusions

The results show that concentrations of constituents in the percent range can be detected in polymer mixtures and, in certain circumstances, even quantified. For the PE-LD/PE-HD system investigated, the detection limit was found to be between 0.5% and 1%.

OIT of polyethylene with the TMA/SDTA840

J. Widmann, Ph. Larbanois

Sample		Crosslinked PE from a plastic pipe (PE-X)
Information expected		OIT, Oxidative Induction Time at 210 °C in oxygen
Measuring conditions	Measuring cell	TMA/SDTA840 with Gas Controller at the reactive gas inlet
	Probe	Negative load of -0.01 N, raised, (no changes in length can be measured with the probe raised)
	Sample preparation	A piece of ca.15 mg was cut off with a knife
	Crucible	Light aluminum pan, 20 µl, with no lid
	TMA measurement	Heating from 50 °C to 210 °C at 20 K/min, then isothermal for 5 min under nitrogen. Afterward, switched to oxygen (gas inlet: reactive gas)

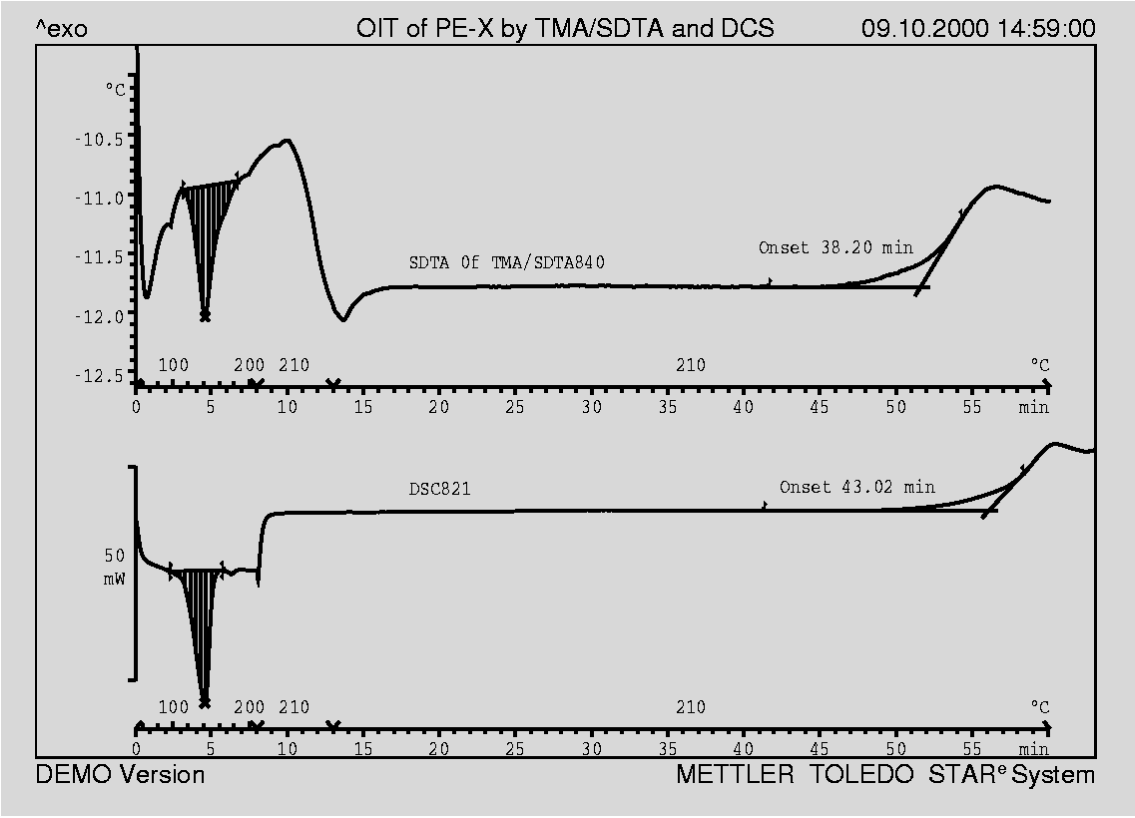

Atmosphere	N2 and O2 50 ml/min, purge gas N2, 20 ml/min
Interpretation	The Oxidative Induction Time evaluated with TA/Onset is 38.5 min (time from switching over to oxygen to the onset). A DSC measurement made for comparison purposes gave a result of 43.4 min. The melting point on the left of the diagram confirms the identity of the sample as PE.
Conclusions	TMA with simultaneous SDTA can easily measure all the relatively strong thermal effects, including the above oxidation reaction. The difference between the values of OIT measured with SDTA and DSC is within the limits of reproducibility of such measurements. It would also be possible to simultaneously perform TMA measurements in the same experiment, e.g. to measure the plastic deformation above the crystallite melting point in order to assess the degree of crosslinking (see Collected Applications, Thermoplastics).

Tips

Effect of sample mass on TG results

Dr. R. Riesen

Introduction

Thermogravimetric Analysis (TGA) measures the change in weight of a sample as a function of temperature. For example, to assess the thermal stability of a sample one would like to know the temperature at which 10% weight loss occurs, or at what rate evaporation or sublimation takes place. To obtain the best possible reproducibility and accuracy in such experiments, it is important to know the effect of measurement parameters such as the type of purge gas and flow rate, the heating rate, and the sample preparation.

One parameter that is very often underestimated in TGA measurements is the effect of sample weight. This parameter has, above all, to do with heat transfer from the furnace to the sample. All evaporation and (endothermic) decomposition processes require a supply of energy. In the TG furnace, heat is transferred to the sample through convection (which predominates at low temperatures) and radiation (which predominates at high temperatures). A small sample therefore decomposes much more rapidly than a large sample, which means that the end of the TG step is reached earlier and therefore at lower temperatures. Besides this, larger samples generate more gas. This has to escape through pores in the sample and from the crucible, thereby prolonging the effect.

The effects described above are illustrated in the following example, without going into other effects such as sample geometry or sample density.

Experimental

Decabromodiphenyloxide DECA ($C_{12}Br_{10}O$, molecular weight 959.2, density 3.0 g/ml) melts between 300 °C to 305 °C, followed by evaporation (vapor pressure $6.5 \cdot 10^2$ Pa at 360 °C) and decomposition above 400 °C. The substance is used as a flame retardant in plastics and fibers.

The TG measurements were performed with a TGA/SDTA851^e (small furnace) using nitrogen at 50 ml/min as purge gas. The finely powdered samples were heated from 200 °C to 510 °C at 10 K/min in a 70 µl alumina crucible. Whenever other parameters were used, this is mentioned in the text.

The DTG curves are calculated as derivatives of the TG curves. The SDTA curves were determined as the temperature difference between the measured sample temperature and the program temperature.

Results

Effect of sample mass

On heating, the sample of DECA first melts and then immediately begins to lose weight before evaporating completely. The rate at which this takes place depends primarily on the amount of sample. Figure 1 shows the TG curves of five different samples. The weight loss for all five samples, measured in milligrams, begins at the same temperature and with similar rates. The evaporation rates (in mg/min) of the large samples do not become faster until about 380 °C (see also Fig. 2). It is apparent that the smallest sample has already completely evaporated at 400 °C. If the weight loss curves are compared in a normalized presentation (i.e. in % as a function of °C), then the evaporation rates look quite different. For example, a weight loss of 10% occurs for the smallest sample at 337 °C but for the largest not until 8 minutes later (at 403 °C). This time difference occurs because much more heat is needed to vaporize 3.3 mg than 0.2 mg.

With small sample weights, the TG curves lie exactly on top of each other. Weight loss is however to some extent accelerated with larger sample weights. This can be explained as being the result of surface transport and gas transport properties. It could also be caused by the decomposition reaction beginning to take effect (see below). The SDTA curves in Figure 2 show that larger samples also take longer to melt than smaller samples (melting at 310 °C). The beginning is, however, in agreement with the TG curve, practically independent

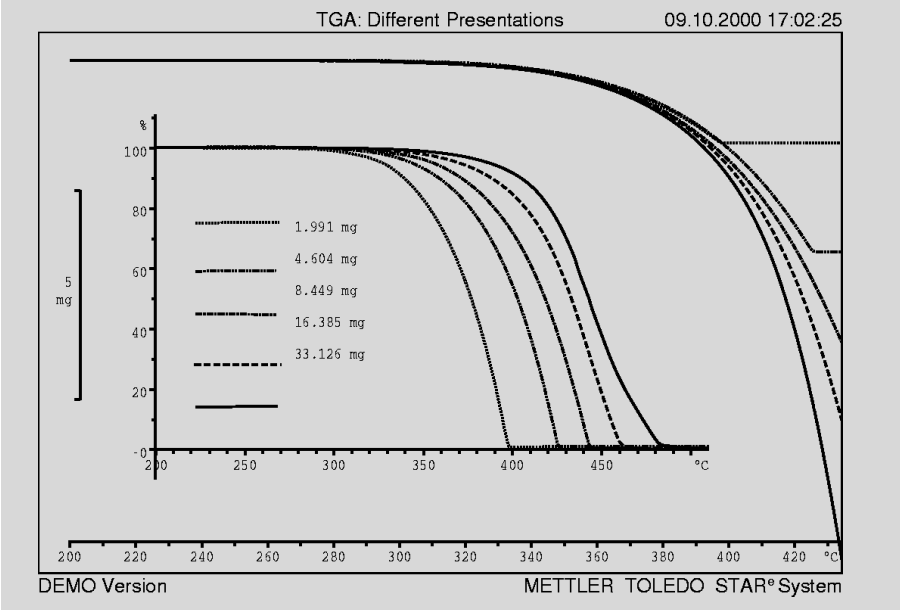

Fig. 1. TG curves of DECA with different sample weights in an open 70 µl alumina crucible. The five measurements are shown in two different presentations: with the ordinate absolute in milligrams (upper curves), and normalized in % with respect to the initial sample weight.

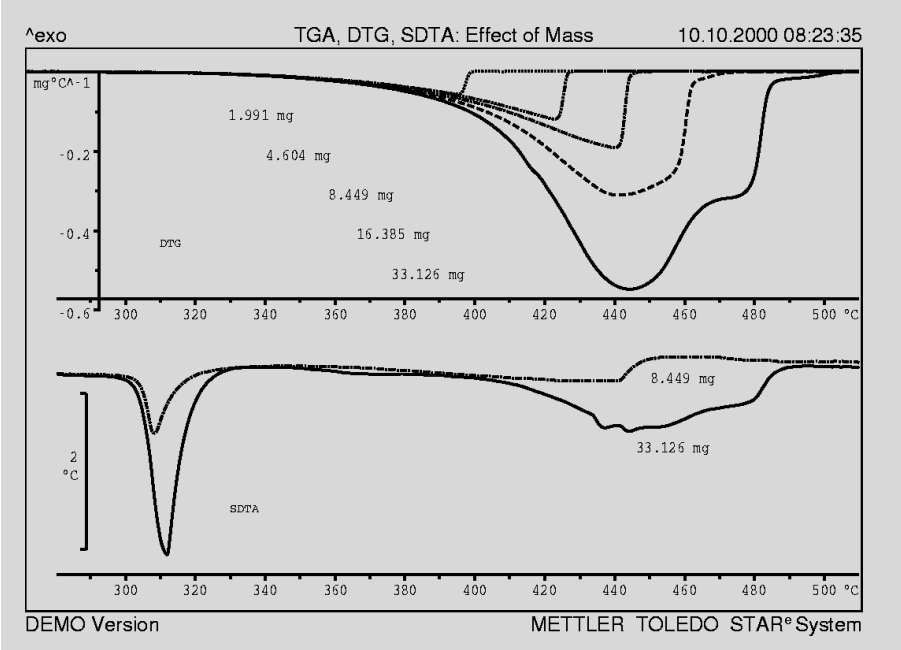

Fig. 2. The DTG curves (calculated from the absolute sample weight, see the TG curves in Fig. 1) show the evaporation rates for various sample weights in a standard open crucible. SDTA curves are also shown for sample weights of 8 mg and 33 mg.

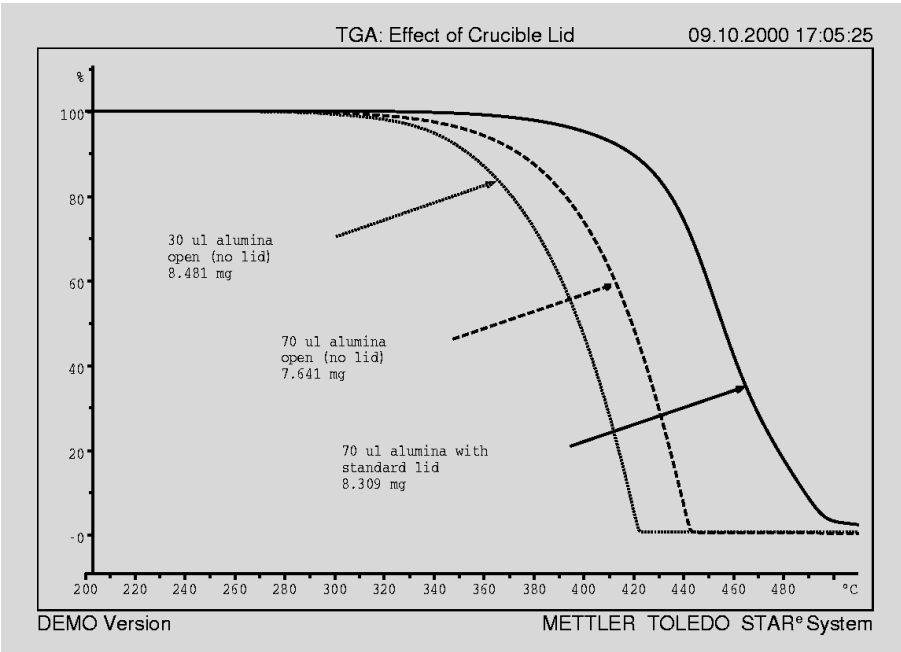

Fig. 3. Evaporation of DECA in different crucibles. Dotted curve: 30 µl crucible with low rim; dashed curve: crucible with high rim (70 µl alumina crucible); continuous curve: 70 µl crucible with lid (and small hole).

of the sample mass:
onset (8 mg) 304.2 °C,
onset (33 mg) 304.0 °C;
peak (8 mg) 307.9 °C,
peak (33 mg) 309.5 °C.
The SDTA curves in the evaporation range are similar to the DTG curves because the loss of weight is directly related to the uptake of energy.
With large samples, the long evaporation time and the relatively rapid heating rate of 10 K/min means that temperatures are reached at which decomposition begins. This is particularly clear in the DTG curves in Figure 2. The curve shape typical of an evaporation process is visible in the two smallest samples. With larger samples, this curve shape is overlapped by the decomposition reaction, i.e. there is an additional loss of weight, which is indicated by the peak on the evaporation curve. As can be seen in Figure 1 (mg versus °C), the decomposition of the substance already begins at temperatures below 400 °C and is correspondingly stronger with larger samples.

Effect of gas exchange

Sample size and the quantity of energy required for evaporation or decomposition are however not the only factors responsible for a "shift" of the TG curves. Gas exchange and the diffusion of gaseous products also have a large effect. This is illustrated in Figure 3, which shows the measurement of samples of similar (medium) weight using different crucibles. In an open crucible, evaporation is relatively rapid but the delayed removal of vapor from the deep crucible causes the liquid-vapor equilibrium to shift to higher temperatures. This results in the TG curve being recorded at about 20 K higher. If gas exchange is even more restricted (with a lid), the equilibrium is shifted to even higher temperatures by the self-generated atmosphere; the evaporation is therefore overlapped by significant decomposition.

Conclusions

In thermogravimetry, it is essential to keep not only the temperature, but also all the other experimental parameters under precise control. To achieve the best possible reproducibility, it is important to know how these parameters affect the measurement results. As has previously been shown [UserCom 9, p.22], the type of crucible used has a major influence on the rate of gas exchange and hence on the weight loss. For the same reason, the sample weight also influences the temperature observed for an effect, and the rate of weight loss. Even when sample weights are practically identical, a small degree of measurement uncertainty is still to be expected. A series of measurements on samples of the same weight, for example, showed that a temperature deviation of ±1 °C at 10% weight loss is possible because other less important parameters such as sample geometry of the crucible, particle size, packing density, etc. all affect reproducibility. The degree of uncertainty is however much less than the shift of 60 K caused by widely different sample weights.

Exhibitions, Conferences and Seminars - Veranstaltungen, Konferenzen und Seminare

14. Ulm-Freiberger Kalorimetrietage	21 - 23. März 2001	Freiberg, Germany
Pittsburgh Conference	March 4-9, 2001	New Orleans, LA
221st American Chemical Society National Exposition	April 2-4, 2001	San Diego, CA
222nd American Chemical Society National Exposition	Aug. 27-29, 2001	Chicago, IL
MEDICTA 2001	Sept. 2-7, 2001	Jerusalem, Israel
29th Annual North American Thermal Analysis Society Meeting	Sept. 24-26, 2001	St. Louis, MO
ESTAC 8	Aug. 25-29, 2002	Barcelona, Spain

TA Customer Courses and Seminars in Switzerland - Information and Course Registration:
TA Kundenkurse und Seminare in der Schweiz - Auskunft und Anmeldung bei:

Helga Judex, METTLER TOLEDO GmbH, Schwerzenbach, Tel.: ++41-1 806 72 65, Fax: ++41-1 806 72 40, e-mail: helga.judex@mt.com

TMA/DMA (Deutsch)	26. Februar 2001 Greifensee	TMA/DMA (English)	March 5, 2001 Greifensee
STARe SW Workshop Basic (D)	26. Februar 2001 Greifensee	STARe SW Workshop Basic (E)	March 5, 2001 Greifensee
TGA (Deutsch)	27. Februar 2001 Greifensee	TGA (English)	March 6, 2001 Greifensee
DSC Basic (Deutsch)	28. Februar 2001 Greifensee	DSC Basic (English)	March 7, 2001 Greifensee
DSC Advanced (Deutsch)	1. März 2001 Greifensee	DSC Advanced (English)	March 8, 2001 Greifensee
STARe SW Workshop Adv. (D)	2. März 2001 Greifensee	STARe SW Workshop Adv. (E)	March 9, 2001 Greifensee
TMA/DMA (Deutsch)	10. September 2001 Greifensee	TMA/DMA (English)	September 17, 2001 Greifensee
STARe SW Workshop Basic (D)	10. September 2001 Greifensee	STARe SW Workshop Basic (E)	September 17, 2001 Greifensee
TGA (Deutsch)	11. September 2001 Greifensee	TGA (English)	September 18, 2001 Greifensee
DSC Basic (Deutsch)	12. September 2001 Greifensee	DSC Basic (English)	September 19, 2001 Greifensee
DSC Advanced (Deutsch)	13. September 2001 Greifensee	DSC Advanced (English)	September 20, 2001 Greifensee
STARe SW Workshop Adv. (D)	14. September 2001 Greifensee	STARe SW Workshop Adv. (E)	September 21, 2001 Greifensee

TA-Kundenkurse und Seminare (Deutschland)

Für nähere Informationen wenden Sie sich bitte an METTLER TOLEDO GmbH, Giessen: Frau Ina Wolf, Tel.: ++49-641 507 404.

DSC-Kundenkurs	12/13.März 2001 Giessen/D	ADSC-Kundenkurs	14. März 2001 Giessen/D
Workshop Pharma: "TA-Methoden zur QS/QC in der pharmazeutischen F&E und Produktion"			15/16. März 2001 Giessen/D
Seminar "Thermoanalytische -und spektroskopische Methoden an Kunststoffen"			13. September 2001 Darmstadt/D
Workshop Kurveninterpretation 24.Oktober 2001 Giessen/D		DSC-Kundenkurs	22/23. Oktober 2001 Giessen/D

Informations-Tage: Wien(A) 07.03.2001 Nürnberg (D) 27.03.2001 München(D) 03.04.2001
Stuttgart (D) 05.04.2001 Greifensee (CH) 05.04.2001

Cours et séminaires d'Analyse Thermique en France et en Belgique

France: Renseignements et inscriptions par Christine Fauvarque, METTLER TOLEDO S.A.,
Viroflay: Tél.: ++33-1 30 97 16 89, Fax: ++33-1 30 97 16 60.
Belgique: Renseignements et inscriptions par Pat Hoogeras, N.V. METTLER TOLEDO S.A., Lot, Tél.: ++32-2 334 02 09, Fax: ++32 2 334 02 10.

Cours clients:

TGA et logiciel STARe	27 mars 2001	Viroflay (France)	TG et logiciel STARe	16 octobre 2001	Viroflay (France)
DSC et logiciel STARe	28 mars 2001	Viroflay (France)	DSC et logiciel STARe	17 octobre 2001	Viroflay (France)
DSC avancé et logiciel STARe	29 mars 2001	Viroflay (France)	DSC avancé et logiciel STARe	18 octobre 2001	Viroflay (France)
TMA et logiciel STARe	30 mars 2001	Viroflay (France)	TMA et logiciel STARe	19 octobre 2001	Viroflay (France)

Journées d'information :

Journée d'information	13 février 2001	Tours (France)	Journée d'information,	19 juin 2001	Aix (France)
Journée d'information,	3 avril 2001	Amiens (France)	Journée d'information,	25 septembre 2001	Nancy (France)
Journée d'information,	29 mai 2001	Pau (France)	Journée d'information,	20 novembre 2001	Nantes (France)

Séminaires:

Aspects de Cinétique en Thermo-Analyse 16 janvier 2001 Toulouse (France)
avec la participation du Prof. N. Sbirrazzuoli, Laboratoire de thermodynamique Expérimentale, Université de Nice/Sophia-Antipolis.
Analyse Thermique, principes de base et méthodes d'investigation sur des échantillons inconnus 13 mars 2001 Lyon (France)
avec la participation de Mr Létoffé, Ingénieur INSA, Laboratoire de Thermodynamique Appliquée, INSA de Lyon.
DSC Alternative et ses applications 23 octobre 2001 Paris La Défense (France)
avec la participation de Dr. M. Ribeiro, Laboratoire de Thermodynamique et Génie Chimique du Prof. Grolier, LTGC de Clermont-Ferrand.

TA Information Day	10 Octobre 2001	Bruxelles (Belgique)
STARe User Forum	11 Octobre 2001	Bruxelles (Belgique)

Corsi e Seminari di Analisi Termica per Clienti in Italia

Per ulteriori informazioni prego contattare: Simona Ferrari
METTLER TOLEDO S.p.A., Novate Milanese, Tel.: ++39-2 333 321, Fax: ++39-2 356 2973.

Corsi per Clienti:

DSC base	6 Marzo,	5 Giugno,	18 Settembre 2001	Novate Milanese
DSC avanzato	7 Marzo,	6 Giugno,	19 Settembre 2001	Novate Milanese
TGA	8 Marzo,	7 Giugno,	20 Settembre 2001	Novate Milanese
TMA	9 Marzo,	8 Giugno,	21 Settembre 2001	Novate Milanese

Giornate di informazione (Caratterizzazione dei Materiali)

Milano	1 Marzo 2001	Bologna	27 Marzo 2001
Napoli	20 Marzo 2001	Venezia	28 Marzo 2001
Roma	21 Marzo 2001	Torino	29 Marzo 2001
Firenze	22 Marzo 2001		

Seminario di Analisi Termica (Polimeri) 11 Aprile 2001 Milano

Cursos y Seminarios de TA en España

Para detalles acerca de los cursos y seminarios, por favor, contacte con: Francesc Catala en Mettler-Toleo S.A.E., Tel: ++34 93 223 76 00
E-mail: francesc.catala@mt.com

Jornadas de Análisis Térmico

Sevilla 13-feb-01	Granada 15-feb-01	Zaragoza 3-abr-01
Valencia 5-abr-01	Bilbao 5-jun-01	Santiago de Compostela 7-jun-01

Seminarios de Análisis Térmico

Jornada TA de aplicationes a Polimeros	16-oct-01 Madrid	23-oct-01 Barcelona
Jornada TA para Usuarios del Sistema STARe	17-oct-01 Madrid	24-oct-01 Barcelona
Jornada TA de applicaciones a Farmacia y Quimica	18-oct-01 Madrid	25-oct-01 Barcelona

TA Customer Courses and Seminars in the USA and Canada

Basic Thermal Analysis Training based upon the STARe System version 6 is being offered in California and at Columbus, Ohio Headquarters. Training will include lectures and hands-on workshops.
For information contact Jon Foreman at 1-800-638-8537 extension 4687 or by e-mail jon.foreman@mt.com

TA course	April 17 - 18, 2001	Columbus (OH)
TA course	October 10 - 11, 2001	Columbus (OH)

TA Customer Courses and Seminars in Japan

For details of training courses and seminars please contact:
Yasushi Ikeda at METTLER TOLEDO Japan, Tel.: +81-3-5762-0606; Facsimile: +81-3-5762-0756

Basic course STARe February 22, 2001 Tokyo	Basic course STARe May 25, 2001 Osaka
Advanced course STARe September 14, 2001 Tokyo	Advanced course STARe November 15, 2001 Osaka
TA information day February 24, 2001 Tokyo	TA information day October 25, 2001 Osaka

For further information regarding meetings, products or applications please contact your local METTLER TOLEDO representative.
Bei Fragen zu weiteren Tagungen, den Produkten oder Applikationen wenden Sie sich bitte an Ihre lokale METTLER TOLEDO Vertretung.
Internet: http:/www.mt.com

Editorial team

METTLER TOLEDO GmbH, Analytical, Sonnenbergstrasse 74, CH-8603 Schwerzenbach, Schweiz






Dr. M. Schubnell, Physicist
Dr. R. Riesen, Chemical Engineer
J. Widmann, Chemical Engineer
Dr. J. Schawe, Physicist
C. Darribère, Chemical Engineer
U. Jörimann Electrical Engineer
e-mail: urs.joerimann@mt.com, Tel.: ++41 1 806 73 87, Fax: ++41 1 806 72 60

Layout und Production

Promotion & Dokumentation Schwerzenbach, G. Unterwegner ME-51710054

Printed on 100% chlorine-free paper, for the sake of the environment.